Molecular Pharmacology Fast Forward. Published on February 18, 2021 as DOI: 10.1124/molpharm.120.000185
This article has not been copyedited and formatted. The final version may differ from this version.

Positive allosteric modulators of metabotropic glutamate receptor 5 as tool compounds to study signaling bias

Angela Arsova[1], Thor C. Møller[1], Shane D. Hellyer, Line Vedel, Simon R. Foster, Jakob L. Hansen, Hans Bräuner-Osborne[2] and Karen J. Gregory[2]

Department of Drug Design and Pharmacology, Faculty of Health and Medical Sciences, University of Copenhagen, Universitetsparken 2, 2100 Copenhagen, Denmark (A.A., T.C.M., L.V., S.R.F., and H.B.-O.); Drug Discovery Biology, Monash Institute of Pharmaceutical Sciences and Department of Pharmacology, Monash University, Parkville, VIC, Australia (S.D.H. and K.J.G.); and Cardiovascular Research, Novo Nordisk A/S, Novo Nordisk Park 1, 2760 Måløv, Denmark (J.L.H.). Current address for S.R.F: QIMR Berghofer Medical Research Institute, Brisbane 4006, QLD, Australia.

Molecular Pharmacology Fast Forward. Published on February 18, 2021 as DOI: 10.1124/molpharm.120.000185
This article has not been copyedited and formatted. The final version may differ from this version.

Running title: Positive allosteric modulation of the $mGlu_5$ receptor

Corresponding authors:

Name: Karen J. Gregory

Address: 381 Royal Parade, Parkville, VIC, Australia, 3052

Telephone: +61 399039243

Email: karen.gregory@monash.edu

Name: Hans Bräuner-Osborne

Address: Universitetsparken 2, 2100 Copenhagen, Denmark

Telephone: +45 35334469

Email: hbo@sund.ku.dk

Text pages: 54

Tables: 5

Figures: 8

References: 59

Words in Abstract: 230

Words in Introduction: 743

Words in Discussion: 1754

Nonstandard abbreviations: AM, acetoxymethyl; BCA, bicinchoninic acid; CDPPB, 3-cyano-N-(2,5-diphenylpyrazol-3-yl)benzamide; compound 2c, 1-[4-(4-chloro-2-fluoro-phenyl)piperazin-1-yl]-2-(4-pyridylmethoxy)ethenone; CPCCOEt, 7-

Molecular Pharmacology Fast Forward. Published on February 18, 2021 as DOI: 10.1124/molpharm.120.000185
This article has not been copyedited and formatted. The final version may differ from this version.

(hydroxyimino)cyclopropa[b]chromen-1a-carboxylate ethyl ester; CPPZ, 1-(4-(2-chloro-4-fluorophenyl)piperazin-1-yl)-2-(pyridin-4-ylmethoxy)ethenone; dFBS, dialyzed FBS; DHPG, (*S*)-3,5-dihydroxyphenylglycine; DL-TBOA, DL-*threo*-β-benzyloxyaspartic acid; DMEM, Dulbecco's modified Eagle medium; EAAT3, excitatory amino acid transporter 3; ERK1/2, extracellular signal-regulated kinase 1/2; FBS, fetal bovine serum; FRET, Förster resonance energy transfer; GPT, glutamic-pyruvic transaminase; GPCR, G protein-coupled receptor; HA, hemagglutinin; HBSS, Hank's balanced salt solution; HEK293A, human embryonic kidney 293A; IP_1, inositol monophosphate; LY341495, (1S,2S)-2-[(1S)-1-amino-1-carboxy-2-(9H-xanthen-9-yl)ethyl]cyclopropane-1-carboxylic acid; methoxy-PEPy, 3-methoxy5-(2-pyridinylethynyl)pyridine; $mGlu_5$, metabotropic glutamate type 5; MPEP, 2-methyl-6-(phenylethynyl)pyridine hydrochloride; MPPA, *N*-methyl-5-(phenylethynyl)pyrimidin-2-amine; NMDA, N-methyl D-aspartate receptor; RFU, relative fluorescence units; PAM, positive allosteric modulator; VU0403602, *N*-cyclobutyl-5-((3-fluorophenyl)ethynyl)picolinamide; VU0424465, 5-[2-(3-fluorophenyl)ethynyl]-N-[(2R)-3-hydroxy-3-methylbutan-2-yl]pyridine-2-carboxamide

Molecular Pharmacology Fast Forward. Published on February 18, 2021 as DOI: 10.1124/molpharm.120.000185
This article has not been copyedited and formatted. The final version may differ from this version.

Abstract

Positive allosteric modulation of metabotropic glutamate type 5 ($mGlu_5$) receptor has emerged as a potential new therapeutic strategy for the treatment of schizophrenia and cognitive impairments. However, positive allosteric modulator (PAM) agonist activity has been associated with adverse side effects, and neurotoxicity has also been observed for pure PAMs. The structural and pharmacological basis of therapeutic vs adverse $mGlu_5$ PAM *in vivo* effects remains unknown. Thus, gaining insights into the signaling fingerprints, as well as the binding kinetics of structurally diverse $mGlu_5$ PAMs, may help in the rational design of compounds with desired properties. We assessed the binding and signaling profiles of *N*-methyl-5-(phenylethynyl)pyrimidin-2-amine (MPPA), 3-cyano-N-(2,5-diphenylpyrazol-3-yl)benzamide (CDPPB), and 1-[4-(4-chloro-2-fluoro-phenyl)piperazin-1-yl]-2-(4-pyridylmethoxy)ethenone (compound 2c, a close analogue of 1-(4-(2-chloro-4-fluorophenyl)piperazin-1-yl)-2-(pyridin-4-ylmethoxy)ethanone (CPPZ)) in human embryonic kidney 293A (HEK293A) cells stably expressing $mGlu_5$ using Ca^{2+} mobilization, inositol monophosphate (IP_1) accumulation, extracellular signal-regulated kinase 1/2 (ERK1/2) phosphorylation, and receptor internalization assays. Of the three allosteric ligands, only CDPPB had intrinsic agonist efficacy and also had the longest receptor residence time and highest affinity. MPPA was a biased PAM, showing higher positive cooperativity with orthosteric agonists in ERK1/2 phosphorylation and Ca^{2+} mobilization over IP_1 accumulation and receptor internalization. In primary cortical neurons, all three PAMs showed stronger positive cooperativity with DHPG in Ca^{2+} mobilization over IP_1 accumulation. Our characterization of three structurally diverse $mGlu_5$ PAMs provides further molecular pharmacological insights and presents the first assessment of PAM-mediated $mGlu_5$ internalization.

Molecular Pharmacology Fast Forward. Published on February 18, 2021 as DOI: 10.1124/molpharm.120.000185
This article has not been copyedited and formatted. The final version may differ from this version.

Molecular Pharmacology Fast Forward. Published on February 18, 2021 as DOI: 10.1124/molpharm.120.000185
This article has not been copyedited and formatted. The final version may differ from this version.

Significance Statement

Enhancing metabotropic glutamate receptor subtype 5 ($mGlu_5$) activity is a promising strategy to treat cognitive and positive symptoms in schizophrenia. It is increasingly evident that positive allosteric modulators (PAMs) of $mGlu_5$ are not all equal in preclinical models; there remains a need to better understand the molecular pharmacological properties of $mGlu_5$ PAMs. Here, we report detailed characterization of the binding and functional pharmacological properties of $mGlu_5$ PAMs, including the first study of the effects of $mGlu_5$ PAMs on receptor internalization.

Molecular Pharmacology Fast Forward. Published on February 18, 2021 as DOI: 10.1124/molpharm.120.000185
This article has not been copyedited and formatted. The final version may differ from this version.

Introduction

The involvement of metabotropic glutamate (mGlu) receptors in central nervous system (CNS) disorders such as Parkinson's disease, schizophrenia and major depressive disorder has made these receptors interesting targets for drug discovery research (Foster and Conn, 2017; Nicoletti et al., 2015). Metabotropic glutamate receptor 5 ($mGlu_5$) is a group I mGlu receptor that is primarily coupled to $G_{q/11}$ proteins. $mGlu_5$ is generally found post-synaptically and is important in neuronal development and synaptic plasticity; for instance in memory formation and cognition (Dhami and Ferguson, 2006; Valenti et al., 2002; Waung and Huber, 2009). High sequence similarity in the orthosteric glutamate binding site between the eight mGlu receptor subtypes makes the discovery of selective orthosteric ligands challenging (Wellendorph and Bräuner-Osborne, 2009). Hence, $mGlu_5$ discovery efforts have focused on targeting topographically distinct sites with allosteric modulators; many diverse scaffolds have been identified that interact with a common site within the seven-transmembrane domains (Christopher et al., 2018; Dore et al., 2014). Allosteric modulators offer higher subtype receptor selectivity, the ability to spatiotemporally regulate pre-existing receptor responses and, in this way, potentially avoid unwanted side-effects (Changeux and Christopoulos, 2017; Melancon et al., 2012). Allosteric modulators may enhance (termed positive allosteric modulators; PAMs), or diminish receptor activation (termed negative allosteric modulators; NAMs) (Gentry et al., 2015). PAMs can have intrinsic agonist activity and are referred to as PAM-agonists (Foster and Conn, 2017; Sengmany et al., 2017).

The first bioavailable $mGlu_5$ PAM, 3-cyano-N-(1,3-diphenyl-1H-pyrazol-5-yl)benzamide (CDPPB), had anti-psychotic-like and pro-cognitive effects in preclinical models, establishing $mGlu_5$ PAMs as promising interventions for schizophrenia (Horio et al., 2013; Kinney et al., 2005). Subsequently, $mGlu_5$ PAMs have also been associated with serious adverse effects

Molecular Pharmacology Fast Forward. Published on February 18, 2021 as DOI: 10.1124/molpharm.120.000185
This article has not been copyedited and formatted. The final version may differ from this version.

such as neurotoxicity and seizure induction (Bridges et al., 2013; Parmentier-Batteur et al., 2014; Rook et al., 2013). These adverse side effects were initially attributed to PAM-agonist activity, e.g. VU0424465 (Rook et al., 2013) and VU0403602 (Bridges et al., 2013). However, some pure PAMs may also lead to neurotoxicity, indicating that PAM-agonist activity is not the only predictor of adverse effect liability (Parmentier-Batteur et al., 2014). In many drug discovery paradigms, PAM-agonist activity is only tested in a single functional assay (i.e. Ca^{2+} mobilization). Such approaches do not detect pleiotropic $mGlu_5$ signaling; therefore some "pure" PAMs may in fact be agonists for different cellular responses. Investigation of biased $mGlu_5$ signaling has thus emerged as a means to avoid unwanted side effects (Sengmany et al., 2017). Relative to a reference agonist, a "biased agonist" preferentially activates select responses relative to others activated through the same receptor (Trinh et al., 2018). Biased agonism is believed to be achieved through the stabilization of unique receptor conformations, that have higher affinity for certain effector proteins over others (Kenakin and Christopoulos, 2013; Smith et al., 2018). Biased allosteric modulation is also possible, manifesting as different apparent affinities or magnitudes of cooperativity with the same orthosteric agonist depending upon the response measured (Hellyer et al., 2019; Sengmany et al., 2019; Sengmany et al., 2017).

Alongside the conformational theory for ligand bias, ligand binding kinetics are also implicated in signaling bias (Klein Herenbrink et al., 2016; Lane et al., 2017). The duration of the ligand-receptor complex is proposed to be proportional to agonist efficacy (Copeland, 2016); compounds occupying receptors longer potentially catalyze more effector protein activation cycles (Lane et al., 2017). Therefore, increasing receptor residence time has been exploited as a strategy in rational drug design to increase ligand affinity and efficacy (Lindstrom et al., 2007; Tummino and Copeland, 2008). However, long residence times may

Molecular Pharmacology Fast Forward. Published on February 18, 2021 as DOI: 10.1124/molpharm.120.000185
This article has not been copyedited and formatted. The final version may differ from this version.

also lead to on-target toxicity (Kapur and Seeman, 2001). To date, the contribution of ligand binding kinetics to $mGlu_5$ biased agonism and potentiation has remained unexplored.

Here, we evaluated the signaling profiles of three structurally diverse $mGlu_5$ PAMs using four different functional assays: Ca^{2+} mobilization, IP_1 accumulation, ERK1/2 phosphorylation, and real-time receptor internalization. N-methyl-5-(phenylethynyl)pyrimidin-2-amine (MPPA) is a potent PAM of glutamate stimulation of intracellular Ca^{2+} mobilization and has efficacy in reversing amphetamine-induced hyperlocomotion in rats (Sharma et al., 2009). Discovered alongside the *in vivo* efficacious PAM CPPZ, compound 2c has previously only been evaluated as a PAM of glutamate in $mGlu_5$-Ca^{2+} mobilization assays (Xiong et al., 2010). The intrinsic efficacy and potentiation (of DHPG and L-glutamate) by these two PAMs were compared to CDPPB, a well-characterized PAM-agonist of glutamate activation of $mGlu_5$ (Kinney et al., 2005; Sengmany et al., 2017). Moreover, we determined kinetics of PAM binding to $mGlu_5$, and compared these parameters to affinity estimates obtained with functional assays and inhibition binding experiments.

Molecular Pharmacology Fast Forward. Published on February 18, 2021 as DOI: 10.1124/molpharm.120.000185
This article has not been copyedited and formatted. The final version may differ from this version.

Materials and Methods

The experiments presented in this paper were planned based on the availability of compounds and established assays and cell lines in the two laboratories where the experiments were performed. The experiments were exploratory (i.e. not designed to test a prespecified statistical null hypothesis) and the reported P-values should therefore be viewed as descriptive. The minimum number of independent experiments was decided beforehand based on our previous experiences with the assays and cell lines.

Materials. MPPA, CDPPB and compound 2c were obtained from Lundbeck (Copenhagen, Denmark). DHPG, CPCCOEt, MPEP, LY341495 and DL-TBOA were purchased from Tocris (Bristol, UK). DMEM GlutaMAX-I, fetal bovine serum (FBS), dialyzed FBS (dFBS) penicillin-streptomycin solution, B-27, Fungizone antimycotic, Neurobasal media, Fluo-4 AM cell permeant dye, and HBSS were purchased from Invitrogen (Carlsbad, CA). Probenecid, Pierce BCA Protein Assay kit, and Fluo-4 AM no wash kit were purchased from Thermo Fisher Scientific (Waltham, MA). [^{3}H]methoxy-PEPy was custom synthesized by Pharmaron (Manchester, UK). MicroScint-20 was purchased from PerkinElmer (Waltham, MA). pRK5 plasmids encoding HA- and SNAP-tagged rat $mGlu_{5a}$ (HA-ST-$rmGlu_{5a}$) and excitatory amino acid transporter 3 (EAAT3) were gifts from Laurent Prézeau (Institut de Génomique Fonctionnelle, Montpellier, France) and previously described (Brabet et al., 1998; Doumazane et al., 2011). All of the other reagents were purchased from Sigma-Aldrich (St. Louis, MO).

Cell culture. Low-expressing wild-type rat $mGlu_5$ ($rmGlu_5$) HEK293A stable cell line (HEK293A-$mGlu_5$-low) was maintained as described previously (Sengmany et al., 2017) or, when cultured in parallel with non-transfected HEK293A cells, DMEM GlutaMAX-I was used and supplemented with 10% dFBS, 1%, penicillin-streptomycin and 16 mM HEPES,

Molecular Pharmacology Fast Forward. Published on February 18, 2021 as DOI: 10.1124/molpharm.120.000185
This article has not been copyedited and formatted. The final version may differ from this version.

where geneticin (500 μg/ml) was included to maintain stable expression of HEK293A-mGlu$_5$-low. Cultured cells were routinely monitored for mycoplasma contamination.

Animals. All animal experiments and procedures were approved by the Monash Institute of Pharmaceutical Sciences Animal Ethics Committee (Protocol no. MIPS.2014.37). Eight-week old Asmu:Swiss outbred female wild-type mice were provided by the Monash Animal Research Platform (Clayton, Victoria, Australia). Animals were humanely sacrificed and E16 mixed sex embryos were recovered for primary cell culture.

Primary cell culture. Cortical neurons were isolated from E16 Asmu:Swiss wild-type mice sacrificed by decapitation. The cortex was isolated and neurons mechanically dissociated in ice-cold HBSS. Cortical neurons were plated on a poly-D-lysine- and FBS-coated transparent clear-bottom 96-well plate in Neurobasal media supplemented with 2 mM L-glutamine, 1 x B-27, 50 U/ml penicillin, 50 mg/ml streptomycin, 1.25 mg/ml Fungizone antimycotic, at a density of 100,000 cells/well. Plates were stored at 37 °C and 5% CO_2 for 6-7 days before experimentation.

Radioligand binding assays. Membrane preparations from HEK293A-mGlu$_5$-low cells were prepared as described previously (Arsova et al., 2020). Inhibition of [^{3}H]methoxyPEPy (specific activity 85 Ci/mmol) binding assays were equilibrated for 1 h using our previously described approach in a 96-well plate format (Arsova et al., 2020). In this assay format, ligand depletion is not a concern as the total amount of ligand bound as a percentage of radioligand added was well under 10% for all experiments, ranging from 1.1-3.6%. For association binding experiments, compound and [^{3}H]methoxyPEPy were pre-mixed 1:1 and added to the plate at different time points. For dissociation binding experiments, membranes were pre-equilibrated with [^{3}H]methoxyPEPy for 1 h and a saturating concentration of MPEP (1 μM) was added at different time points to determine the radioligand K_{off}. Membranes were

Molecular Pharmacology Fast Forward. Published on February 18, 2021 as DOI: 10.1124/molpharm.120.000185
This article has not been copyedited and formatted. The final version may differ from this version.

harvested through GF/C filter plates using a 96-well FilterMate harvester (PerkinElmer) to separate unbound radioligand. After drying overnight at room temperature, plates were loaded with MicroScint-20 scintillation liquid and incubated at room temperature for 2 h prior to measuring scintillation spectrometry with a MicroBeta^2 microplate counter (PerkinElmer).

Ca^{2+} mobilization assay. Ca^{2+} mobilization in HEK293A-$mGlu_5$-low cells was measured as previously described (Arsova et al., 2020) and represents both release from intracellular stores as well as influx of extracellular Ca^{2+} (Sengmany et al., 2017). PAM potentiation of the response to 100 nM L-glutamate or DHPG was measured in assay buffer (HBSS supplemented with 20 mM HEPES, 1 mM $MgCl_2$, and 1 mM $CaCl_2$ with pH adjusted to 7.4) with 0.1% bovine serum albumin. Intrinsic PAM agonist activity was measured after 3 h incubation in assay buffer supplemented with 10 U/mL glutamic pyruvic transaminase (GPT) and 10mM sodium pyruvate to eliminate ambient glutamate. Cortical neurons were serum-starved for 4 h at 37 °C and 5% CO_2 in starvation media (DMEM with 4500 mg/l glucose, sodium pyruvate, and sodium bicarbonate, without L-glutamine, supplemented with 16 mM HEPES) before assay initiation. Cortical neurons and HEK293A cells were incubated for 1 h with Fluo-4 AM cell permeant dye diluted in calcium assay buffer (assay buffer as above supplemented with 2.5 mM probenecid). Compounds were diluted in calcium assay buffer to 0.3% final DMSO concentration. After dye loading, cells were washed once with calcium assay buffer. Intrinsic PAM-agonist activity was assessed with and without 15 min preincubation with 300 µM LY341495 following dye loading. Fluorescence was measured on a FlexStation1 or Flexstation3 plate reader (Molecular Devices, San Jose, CA) at 37 °C. For cortical neurons, PAMs were added simultaneously with 120 nM DHPG (or vehicle) at t = 20 s and responses measured over 120 s. 500 nM L-glutamate was added during the final 30 s at t = 110 s to confirm neuron integrity. The peak change in fluorescence was determined after

Molecular Pharmacology Fast Forward. Published on February 18, 2021 as DOI: 10.1124/molpharm.120.000185
This article has not been copyedited and formatted. The final version may differ from this version.

applying a 5-point smoothing function and data expressed as a percentage of the DHPG maximal response.

IP_1 accumulation assay. IP_1 accumulation in HEK293A-$mGlu_5$-low cells was measured with the IP-One assay kit (Cisbio, Codolet, France) as previously described after 3 h incubation in IP_1 assay buffer (HBSS supplemented with 20 mM HEPES, 1 mM $MgCl_2$, 1 mM $CaCl_2$, and 40 mM $LiCl_2$ with pH adjusted to 7.4) supplemented with 10 U/mL GPT and 10mM sodium pyruvate to eliminate ambient glutamate (Arsova et al., 2020). Intrinsic PAM agonist activity was measured with and without 30 min preincubation with 300 µM LY341495 prior to PAM addition. Potentiation of orthosteric agonist activity was measured in the presence of 500 nM L-glutamate or DHPG. Cortical neurons were starved for 4 h in starvation media. Compounds were diluted in IP_1 assay buffer to 0.3% final DMSO concentration. Compounds were incubated for 1 h at 37 °C before IP_1 levels were determined.

ERK1/2 phosphorylation assay. ERK1/2 phosphorylation in HEK293A-$mGlu_5$-low cells was measured with either the Advanced phospho-ERK1/2 (Thr202/Tyr204) assay kit (Cisbio) or AlphaScreen SureFire kit as previously described after 3 h incubation in serum-free DMEM supplemented with 10 U/mL GPT and 10mM sodium pyruvate to eliminate ambient glutamate (Arsova et al., 2020; Sengmany et al., 2017). Intrinsic PAM agonist activity (5min stimulation) was measured with and without 30 min preincubation with 300 µM LY341495. Potentiation of orthosteric agonist activity was measured in the presence of 500 nM L-glutamate (5 min stimulation) or DHPG (20 min stimulation).

Receptor internalization assay. $mGlu_5$ internalization in transiently transfected HEK293A cells was measured with a time-resolved FRET assay after labeling the receptor with SNAP-Lumi4-Tb (Cisbio) as previously described (Arsova et al., 2020). Intrinsic PAM agonist activity was measured with and without 30 min preincubation with 300 µM

Molecular Pharmacology Fast Forward. Published on February 18, 2021 as DOI: 10.1124/molpharm.120.000185
This article has not been copyedited and formatted. The final version may differ from this version.

LY341495. Potentiation of orthosteric agonist activity was measured in the presence of 30 μM DL-TBOA (to measure potentiation of glutamate) or 1 μM DHPG.

Data analysis. Data were analyzed using GraphPad Prism software version 8 (San Diego, CA) as previously described (Arsova et al., 2020). Briefly, inhibition binding data were fitted to either a competitive binding model:

$$Y = \text{Bottom} + \frac{\text{Top}-\text{Bottom}}{1+10^{\log[\text{ligand}]-\log IC_{50}}} \quad (1)$$

or to an allosteric binding model:

$$K_{app} = K_D \frac{1+\frac{[\text{modulator}]}{K_B}}{1+\alpha\frac{[\text{modulator}]}{K_B}}$$

$$Y = Y_0 \frac{[\text{radioligand}]+K_D}{[\text{radioligand}]+K_{app}} \quad (2)$$

where K_D is the equilibrium dissociation constant for the radioligand, K_B is the equilibrium dissociation constant for the allosteric modulator and α is the cooperativity factor. In equation 1, the IC_{50} is the concentration of unlabeled inhibitor that reduces binding to 50% of the top and bottom plateaus. The IC_{50} was used to estimate the K_i (equilibrium dissociation constant of the unlabeled inhibitor) using the Cheng-Prusoff equation (Cheng and Prusoff, 1973).

Competition association binding was fitted to the kinetics of competitive binding model:

$$K_A = k_1[\text{radioligand}] + k_2$$

$$K_B = k_3[\text{ligand}] + k_4$$

$$S = \sqrt{(K_A - K_B)^2 + 4k_1k_3[\text{radioligand}][\text{ligand}]}$$

$$K_F = 0.5(K_A + K_B + S)$$

$$K_S = 0.5(K_A + K_B - S)$$

$$Q = B_{max}\frac{K_1[\text{radioligand}]}{K_F - K_S}$$

$$Y = Q\left(\frac{k_4(K_F-K_S)}{K_FK_S} + \frac{k_4-K_F}{K_F}e^{-K_FX} - \frac{k_4-K_S}{K_S}e^{-K_SX}\right) \quad (3)$$

Molecular Pharmacology Fast Forward. Published on February 18, 2021 as DOI: 10.1124/molpharm.120.000185
This article has not been copyedited and formatted. The final version may differ from this version.

where k_1 and k_2 are the radioligand kinetic association and dissociation rates, respectively, k_3 and k_4 are the unlabeled ligand kinetic association and dissociation rates, respectively, and B_{max} is the maximum binding.

Concentration-response curves from functional assays were fitted with a four parameter sigmoidal concentration response curve to derive EC_{50} and E_{max} values:

$$Y = \text{Bottom} + \frac{\text{Top}-\text{Bottom}}{1+10^{(\log EC_{50}-\log[\text{ligand}])n}} \quad (4)$$

Biased agonism was determined by fitting to the operational model of agonism (Black et al., 1985):

$$Y = \text{basal} + \frac{(E_m-\text{basal})\left(\frac{\tau}{K_A}\right)^n [A]^n}{[A]^n\left(\frac{\tau}{K_A}\right)^n + \left(1+\frac{[A]}{K_A}\right)^n} \quad (5)$$

where [A] is the agonist concentration, E_m is the maximal response of the system, n is the transducer slope and τ is the coupling efficiency. System and observation bias were nullified by subtraction of the transduction coefficient $\log(\tau/K_A)$ of a compound from the transduction coefficient of a reference agonist to obtain $\Delta\log(\tau/K_A)$.

Allosteric modulation of L-Glu- and DHPG-mediated responses were fitted to the operational model of allosterism:

$$\text{Response}=\frac{E_m(\tau_A[A](K_B+\alpha\beta[B])+\tau_B[B]K_A)^n}{([A]K_B+K_AK_B+K_A[B]+\alpha[A][B])^n+(\tau_A[A](K_B+\alpha\beta[B])+\tau_B[B]K_A)^n} \quad (6)$$

where K_A and K_B are the equilibrium dissociation constants of the orthosteric ligand and allosteric modulator respectively, α represents affinity cooperativity and β is a scaling factor representing the effect an allosteric modulator has on orthosteric agonist efficacy, [A] and [B] are the concentrations of the orthosteric agonist and the allosteric modulator, respectively. Parameters τ_A and τ_B represent the intrinsic ability of the orthosteric and allosteric ligand, respectively, to activate the receptor, while E_m and n represent the maximal system response and the transducer slope, respectively. K_A for DHPG and L-glutamate were constrained to

Molecular Pharmacology Fast Forward. Published on February 18, 2021 as DOI: 10.1124/molpharm.120.000185
This article has not been copyedited and formatted. The final version may differ from this version.

values obtained from inhibition binding studies (Gregory et al., 2012; Mutel et al., 2000). Affinity cooperativity α was constrained to 1, assuming neutral cooperativity.

Molecular Pharmacology Fast Forward. Published on February 18, 2021 as DOI: 10.1124/molpharm.120.000185
This article has not been copyedited and formatted. The final version may differ from this version.

Results

Affinity, association and dissociation rates for $mGlu_5$ PAM binding. While previous studies show that CDPPB and MPPA bind to the common allosteric MPEP-site on $mGlu_5$ (Chen et al., 2007; Sharma et al., 2009), there is no binding information available for compound 2c. As such, we measured displacement of the radiolabeled MPEP analog [^{3}H]methoxy-PEPy from $mGlu_5$ to provide insight into the binding site of compound 2c and to determine PAM affinity estimates. Membranes from HEK293A cells with low expression of $mGlu_5$ (HEK293A-$mGlu_5$-low) were used, which have comparable $mGlu_5$ expression to cortical astrocytes (Noetzel et al., 2012). MPPA fully displaced the radioligand, consistent with a competitive interaction (Fig. 1). Only partial displacement was observed for CDPPB, which may be due to either non-competitive interaction or solubility limits of the compound (**Fig. 1**). Similarly, due to limited solubility, we were unable to test sufficiently high compound 2c concentrations to determine if it can fully displace the radioligand (**Fig. 1**). Radioligand displacement curves were analyzed to obtain MPPA affinity (pK_I) estimates using a model of competitive binding, while for CDPPB affinity (pK_B) and affinity cooperativity factor (α) estimates were derived using the allosteric ternary complex model (**Table 1**). The compound 2c displacement curve was fitted with both models.

Binding kinetics of $mGlu_5$ PAMs have not previously been assessed but could potentially be linked to different functional profiles. Therefore, the binding kinetics of MPPA, CDPPB, and compound 2c at $mGlu_5$ were assessed with competition association binding experiments (**Table 1)**. Data were fitted to the association competition binding function (Motulsky and Mahan, 1984), using kinetic parameters for [^{3}H]methoxy-PEPy determined previously (k_{off}: 0.14 ± 0.01 min^{-1}; k_{on}: $2.34 \pm 0.46 \times 10^7$ M^{-1} min^{-1}; Arsova et al., 2020) (**Fig. 2**). Both MPPA and compound 2c had fast binding kinetics, prohibiting accurate quantification of k_{off}. Hence,

Molecular Pharmacology Fast Forward. Published on February 18, 2021 as DOI: 10.1124/molpharm.120.000185
This article has not been copyedited and formatted. The final version may differ from this version.

CDPPB had the longest residence time of the three PAMs, which is also reflected in a higher affinity relative to MPPA and compound 2c. MPPA had the fastest k_{on}, followed by CDPPB and compound 2c (**Table 1**).

Intrinsic agonist activity in signaling assays in HEK293A-mGlu$_5$-low cells. MPPA, CDPPB, and compound 2c were assessed for intrinsic agonist activity by measuring mGlu$_5$ activation of Ca^{2+} mobilization (release from intracellular stores and extracellular influx), IP_1 accumulation and ERK1/2 phosphorylation (**Fig. 3**). Each of the three PAMs showed mGlu$_5$ agonist activity across all three measures. DHPG had similar potency (pEC_{50}) in the Ca^{2+} mobilization, IP_1 accumulation, and ERK1/2 phosphorylation assays (**Supplemental Table 1**). We hypothesized that intrinsic agonist activity of PAMs may be due to potentiation of ambient glutamate. Therefore, experiments were repeated in the presence of 300 µM LY341495, a non-selective mGlu orthosteric antagonist (Kingston et al., 1998). Treatment with LY341495 reduced the basal level of IP_1 accumulation to 22.8% of the untreated control, indicative of inverse agonist activity or inhibition of ambient glutamate (Supplemental Fig 1). LY341495 had no effect on basal responses for Ca^{2+} mobilization or ERK1/2 phosphorylation (Supplemental Fig 1). In the presence of LY341495, only CDPPB retained agonist activity for the three measures of mGlu$_5$ activity, indicating that apparent intrinsic agonism for MPPA and compound 2c was most likely due to modulation of ambient glutamate. CDPPB agonism was then compared to that of the orthosteric agonist DHPG. Relative to DHPG, CDPPB was a partial agonist for Ca^{2+} mobilization and ERK1/2 phosphorylation, but achieved the same maximal response as DHPG in the absence of LY341495 in the IP_1 accumulation assay (**Fig. 3, Supplemental Table 2**, **Supplemental Fig. 1**). CDPPB had significantly lower agonist potency in IP_1 accumulation (12-30 fold) when compared to ERK1/2 phosphorylation and Ca^{2+} mobilization (**Supplemental Table 2**, **Supplemental Fig. 1)**.

Molecular Pharmacology Fast Forward. Published on February 18, 2021 as DOI: 10.1124/molpharm.120.000185
This article has not been copyedited and formatted. The final version may differ from this version.

Potentiation of orthosteric agonists in signaling assays in HEK293A-mGlu$_5$-low cells. MPPA, CDPPB and compound 2c were then tested for their ability to potentiate stimulation of mGlu$_5$ by a low concentration of L-glutamate and DHPG in the three signaling assays (**Fig. 4**). All three PAMs potentiated the responses induced by both orthosteric agonists in Ca^{2+} mobilization, IP_1 accumulation and ERK1/2 phosphorylation signaling assays (**Fig. 4**). Concentration-response curves were fitted to quantify PAM potency ($pPAM_{50}$) and the maximum level of potentiation (PAM_{max}) (**Supplemental Table 3**). Compound 2c potentiated the L-glutamate and DHPG responses to the same maximum response as the orthosteric agonists alone in the Ca^{2+} mobilization and IP_1 accumulation assays. Both compound 2c and CDPPB potentiated the L-glutamate and DHPG responses above the orthosteric agonist maximal response in the ERK1/2 phosphorylation assay (**Fig. 4**). Compound 2c had the lowest potency in all three assays, whereas MPPA and CDPPB had similar PAM potencies (**Supplemental Table 3**).

PAMs induce mGlu$_5$ internalization in HEK293A cells. Most GPCRs are regulated by desensitization and internalization upon agonist stimulation (Ferguson, 2001). The mGlu$_5$ receptor is internalized upon stimulation with L-glutamate (Arsova et al., 2020; Levoye et al., 2015) and several PAMs can induce and/or potentiate DHPG-stimulated mGlu$_5$ desensitization of Ca^{2+} mobilization (Hellyer et al., 2019). The ability of MPPA, CDPPB and compound 2c to induce mGlu$_5$ internalization was characterized using a real-time internalization assay. The assay is based on time-resolved FRET between the long lifetime donor fluorophore Lumi4-Tb, covalently attached to a SNAP-tag on cell surface receptors, and the cell-impermeant acceptor fluorophore fluorescein-O'-acetic acid (Foster and Bräuner-Osborne, 2018; Roed et al., 2014). The assay requires N-terminal fusion of mGlu$_5$ with a SNAP-tag therefore HEK293A cells were transiently transfected with SNAP-tagged mGlu$_5$

Molecular Pharmacology Fast Forward. Published on February 18, 2021 as DOI: 10.1124/molpharm.120.000185
This article has not been copyedited and formatted. The final version may differ from this version.

(HEK293A-SNAP-mGlu$_5$), which resulted in mGlu$_5$ expression levels that were ~10 times higher than in the HEK293A-mGlu$_5$-low cell line (Arsova et al., 2020). Cells were co-transfected with the EAAT3 glutamate transporter to reduce the extracellular glutamate concentration during measurements. To measure PAM potentiation of glutamate, glutamate transport was inhibited by adding the non-transportable EAAT3 inhibitor DL-TBOA at the same time as the PAMs. However, inhibition of EAAT3 with a saturating concentration of DL-TBOA (100 µM) resulted in ~0.9 µM extracellular L-glutamate and ~40% of the mGlu$_5$ internalization induced by 100 µM L-glutamate (Arsova et al., 2020). The DL-TBOA concentration was reduced to 30 µM for the L-glutamate potentiation experiments, which resulted in 24% (95% CI 23-25%, n = 3) of the maximum L-glutamate-induced mGlu$_5$ internalization.

DHPG induced a concentration-dependent increase in mGlu$_5$ internalization that reached a plateau around 60 min after agonist addition (**Supplemental Fig. 2**) similar to the previously observed temporal profile for L-glutamate (Arsova et al., 2020). In the absence of added orthosteric agonist or antagonist, CDPPB and compound 2c induced mGlu$_5$ internalization, although to a lower level than that achieved by DHPG (**Fig. 5A-C**). When 300 µM LY341495 was added to block activation by ambient/released L-glutamate, only CDPPB remained a partial agonist for inducing mGlu$_5$ internalization (**Fig. 5D-F**), consistent with intrinsic efficacy in the three signaling assays (**Fig. 3**). LY341495 alone had no effect on the baseline level of internalization (Supplemental Fig. 1). Internalization concentration-response curves were calculated by determining the area under the curves from the 60 min time courses (**Fig. 6**) and fitted to determine the E_{max} and pEC_{50} values (**Supplemental Table 2**). The agonist potency of CDPPB for internalization was >30-fold lower than for Ca^{2+} mobilization and pERK1/2, but within 3-fold of IP_1 accumulation. DHPG potency for internalization was

Molecular Pharmacology Fast Forward. Published on February 18, 2021 as DOI: 10.1124/molpharm.120.000185
This article has not been copyedited and formatted. The final version may differ from this version.

within 4-fold of the three signaling measures. Compound 2c curves were not well defined, precluding the estimation of E_{max} and pEC_{50} values (**Fig. 6A**)

All three PAMs potentiated L-glutamate- and DHPG-induced internalization with kinetics similar to DHPG (**Fig. 5G-L, Supplemental Fig. 3**). Potentiation of both L-glutamate and DHPG by MPPA induced a lower maximum internalization than CDPPB and compound 2c (**Fig. 6C-D**). Similar to the other signaling assays, compound 2c had the lowest $pPAM_{50}$ value of the three PAMs in the internalization assay. CDPPB and compound 2c potentiated to similar or greater levels of internalization compared to each orthosteric ligand alone (**Fig. 6C-D**).

Quantification and comparison of PAM affinity and cooperativity in HEK293A cells. Comparisons of PAM_{max} and $pPAM_{50}$ values between the four measures of $mGlu_5$ function revealed assay-dependent differences for each PAM (**Supplemental Fig 4**), but no evidence for probe dependence when comparing values derived from DHPG versus L-glutamate (**Supplemental Fig 5**). However, PAM_{max} and $pPAM_{50}$ values are assay-dependent composite values comprising allosteric ligand affinity, cooperativity and efficacy. Assay-independent measures of affinity (pK_A or pK_B), intrinsic efficacy (τ) and cooperativity ($\alpha\beta$) can be derived from fitting of concentration response curves of PAMs and a reference agonist to operational models of agonism or allosterism. CDPPB concentration response curves in the presence of LY341495 were fitted with the operational model of agonism, where DHPG was the reference agonist, to determine pK_A and τ for different $mGlu_5$ functional measures (**Table 2**). The apparent pK_A was lower for the internalization pathway than for Ca^{2+} mobilization and ERK1/2 phosphorylation (**Table 2**). However, the model is limited to partial agonists, so for IP_1 accumulation, where CDPPB behaved as a full agonist, we were only able to determine the composite transduction coefficient $\log(\tau/K_A)$. By comparing these with the transduction

Molecular Pharmacology Fast Forward. Published on February 18, 2021 as DOI: 10.1124/molpharm.120.000185
This article has not been copyedited and formatted. The final version may differ from this version.

coefficient of DHPG, we calculated $\Delta\log(\tau/K_A)$ values for each pathway finding that CDPPB did not show any significant bias between functional measures (**Fig. 7A**, **Table 2**).

We used an operational model of allosterism to determine the affinity (pK_B) and cooperativity ($\log\beta$) from concentration response curves of PAM potentiation of either L-glutamate or DHPG (**Tables 3 and 4**). The intrinsic agonist activity (τ) of CDPPB was constrained to the values determined for CDPPB in the presence of LY341495 when fitting the Ca^{2+} mobilization and ERK1/2 phosphorylation curves. Since τ could not be determined for IP_1 accumulation of CDPPB, it was not possible to use the operational model of allosterism to analyze the corresponding potentiation curves. Furthermore, compound 2c potentiated the activity of both orthosteric agonists in IP_1 accumulation and of DHPG in ERK1/2 phosphorylation above the maximum response of the orthosteric agonist. This prohibited fitting compound 2c data with the operational model of allosterism as there was no independent means to estimate the maximal system response (E_m). With the assumption that PAMs were neutral with respect to affinity cooperativity ($\log\alpha$), comparing the efficacy cooperativity scaling factor ($\log\beta$) across the four functional pathways showed that $\log\beta$ was highest in the Ca^{2+} mobilization pathway for MPPA with L-glutamate, and for the Ca^{2+} mobilization and ERK1/2 phosphorylation pathways for MPPA with DHPG (**Fig. 7B**). The pK_B values were in general agreement between each functional measure and with pK_I values derived from radioligand inhibition binding, although the pK_B values for CDPPB and compound 2c derived from internalization experiment were 5-8-fold lower than the corresponding pK_I values (**Supplemental Fig. 6**). There was no indication of probe bias when comparing the pK_B values obtained in presence of L-glutamate and DHPG, but the $\log\beta$ values were on average 2.09 (95% CI 1.70-2.48) fold higher in presence of DHPG (**Supplemental Fig. 5, C and D**).

Molecular Pharmacology Fast Forward. Published on February 18, 2021 as DOI: 10.1124/molpharm.120.000185
This article has not been copyedited and formatted. The final version may differ from this version.

Agonism and potentiation of DHPG in cortical neurons. We used primary cortical neurons to study PAM Ca^{2+} mobilization and IP_1 accumulation in cells with endogenous expression of $mGlu_5$. In these experiments, we used DHPG as the orthosteric agonist (pEC_{50} values given in **Supplemental Table 1**), as glutamate was unsuitable due to the presence of other mGlu receptors and ionotropic glutamate receptors in cortical neurons. We pre-incubated cells with 30 μM CPCCOEt in order to inhibit activation of $mGlu_1$, which is also a receptor for DHPG (Ito et al., 1992). In the absence of orthosteric ligand, only compound 2c induced a weak agonist response in Ca^{2+} mobilization (**Fig. 8A**). In contrast, all PAMs acted as partial agonists (50-60% of the maximum DHPG response) in the IP_1 accumulation assay (**Fig. 8B**, **Supplemental Table 3**). Although neurons endogenously express glutamate transporters, it is possible that glutamate released during the IP_1 accumulation experiment could contribute to the observed stimulation, similar to what we observed in HEK293A cells, where it was necessary to block the orthosteric binding site with a competitive antagonist to determine the agonist activity of the PAMs. However, there are no $mGlu_5$-selective orthosteric antagonists and, since cortical neurons also express other mGlu receptors, the inclusion of a non-selective orthosteric antagonist such as LY341495 could be a further confounding factor. GPT was included to minimize the influence of ambient glutamate.

All PAMs potentiated a low concentration (120 nM) of DHPG-stimulated $mGlu_5$- Ca^{2+} mobilization and IP_1 accumulation (**Fig. 8, C and D**). In Ca^{2+} mobilization assays, the maximum response of compound 2c potentiation of DHPG (E_{max}) was similar to the E_{max} of DHPG, whereas MPPA and CDPPB induced 40-50% of the DHPG E_{max} (**Supplemental Table 3**). In the IP_1 accumulation pathway, all three PAMs potentiated the DHPG response to 70-80% of the DHPG E_{max} (**Fig. 8D**). CDPPB had the highest potency ($pPAM_{50}$) in both

Molecular Pharmacology Fast Forward. Published on February 18, 2021 as DOI: 10.1124/molpharm.120.000185
This article has not been copyedited and formatted. The final version may differ from this version.

assays in the presence of DHPG and the highest pEC_{50} in the IP_1 accumulation assay without added agonist.

Again, we used operational models to derive the affinities (pK_A) and transduction coefficients $\log(\tau/K_A)$ from PAM concentration response curves in the absence of orthosteric ligand and the affinities (pK_B) and cooperativities ($\log\beta$) from DHPG potentiation curves (**Table 5**). Only compound 2c elicited a response in both pathways in the absence of orthosteric ligand, with similar transduction coefficients for the Ca^{2+} mobilization and IP_1 accumulation pathways. In the presence of DHPG, the cooperativity factors ($\log\beta$) of MPPA, CDPPB and compound 2c were indistinguishable from 0 in the IP_1 accumulation pathway. Therefore, $\log\beta$ was higher for all three PAMs in the Ca^{2+} mobilization pathway. Affinity estimates (pK_B) were similar for the two pathways for MPPA, CDPPB and compound 2c (**Table 5**).

Molecular Pharmacology Fast Forward. Published on February 18, 2021 as DOI: 10.1124/molpharm.120.000185
This article has not been copyedited and formatted. The final version may differ from this version.

Discussion

Positive allosteric modulation of $mGlu_5$ shows promise as a potential therapeutic strategy for schizophrenia. However, undesirable on-target side effects associated with $mGlu_5$ PAMs have stalled development (Foster and Conn, 2017; Parmentier-Batteur et al., 2014; Rook et al., 2013). Development of safer and more efficacious $mGlu_5$ PAMs is hampered by the lack of in-depth molecular pharmacological characterization to accurately link *in vitro* profiles to *in vivo* effects. We provided a detailed characterization of the $mGlu_5$ PAMs CDPPB, MPPA and compound 2c, representing distinct structural scaffolds; MPPA and compound 2c had previously only been assessed in $mGlu_5$-mediated Ca^{2+} mobilization assays. CDPPB had a longer receptor residence time than either MPPA or compound 2c, which correlated with higher $mGlu_5$ affinity. In addition to rigorously profiling the agonist and potentiator activity of each modulator at three measures of acute $mGlu_5$ signaling, for the first time we assessed the influence of $mGlu_5$ PAMs on receptor internalization. We found no evidence for biased agonism; however, MPPA was a biased modulator, with different magnitudes of positive cooperativity with L-glutamate or DHPG depending on the measure of $mGlu_5$ function. Importantly, this biased cooperativity also translated to natively expressed $mGlu_5$ in primary cortical neurons.

Ligand binding kinetics have been correlated with compound affinity and efficacy *in vivo* (Copeland, 2016; Tummino and Copeland, 2008). We report the first assessment of $mGlu_5$ PAM binding kinetics. CDPPB has the longest receptor residence time of the three PAMs. A slower rate of dissociation may be linked to the fact that CDPPB alone showed intrinsic efficacy at all four measures of $mGlu_5$ activity in recombinant cells. For some GPCRs, compounds with longer residence times or fast k_{on} rates have higher efficacy, and thus, have

Molecular Pharmacology Fast Forward. Published on February 18, 2021 as DOI: 10.1124/molpharm.120.000185
This article has not been copyedited and formatted. The final version may differ from this version.

been considered as more desirable lead compounds (Doornbos et al., 2017; Guo et al., 2014; Vauquelin and Charlton, 2010). Indeed, the efficacy (but not affinity) of select $mGlu_2$ PAMs correlate with residence time, whereas increased k_{on} rates correlated with increased affinities (Doornbos et al., 2017). Indeed, MPPA behaved similarly here; a fast k_{on} rate compensated for a short residence time, giving rise to sub-micromolar affinity. Ligand kinetics can also determine the extent of signaling bias for the serotonin 5-HT_{2B} and the dopamine D_2 receptors (Klein Herenbrink et al., 2016; Unett et al., 2013), but not for the μ opioid receptor (Pedersen et al., 2020). In the future, it would be of interest to explore the relationship between receptor residence time and PAM-agonist efficacy and biased agonism for additional structurally diverse $mGlu_5$ ligands.

CDPPB alone retained PAM-agonist activity across all four measures of $mGlu_5$ activity in the presence of both GPT/EAAT3 and LY341495 to negate the confounding influence of ambient glutamate. These data are in keeping with previous evidence for CDPPB PAM-agonist activity as well as induction of receptor desensitization and tolerance development with respect to changes in sleep architecture, although such effects are known to be context and model dependent (Hellyer et al., 2019; Kinney et al., 2005; Parmentier-Batteur et al., 2012). CDPPB showed robust agonist efficacy for IP_1 accumulation, while being a weak partial agonist for Ca^{2+} mobilization and ERK1/2 phosphorylation, consistent with previous work (Sengmany et al., 2017). Application of the operational model of agonism found that CDPPB was not biased relative to DHPG, in direct contrast to earlier findings, where CDPPB and a number of structurally diverse $mGlu_5$ PAMs preferentially activated IP_1 accumulation over Ca^{2+} mobilization relative to L-glutamate or DHPG (Hellyer et al., 2018; Sengmany et al., 2017). One possible explanation for this discrepancy may be the inclusion of the orthosteric antagonist, LY341495. Notably, the same concentration of LY341495 had very

Molecular Pharmacology Fast Forward. Published on February 18, 2021 as DOI: 10.1124/molpharm.120.000185
This article has not been copyedited and formatted. The final version may differ from this version.

different effects on the DHPG concentration-response curve, right shifting DHPG potency in Ca^{2+} mobilization as expected for a competitive antagonist, however, the DHPG response was completely abolished in IP_1 accumulation and pERK1/2. Moreover, LY341495 markedly reduced basal IP_1 accumulation, suggestive of inverse agonist activity. The lack of apparent inverse agonism for other $mGlu_5$ activity measures may reflect observational bias or an LY341495 specific effect. Certain $mGlu_5$ NAMs are biased modulators (Arsova et al., 2020; Jong et al., 2019; Sengmany et al., 2019); future experiments should explore this possibility for orthosteric antagonists. Therefore, it is possible that the receptor conformations sampled when simultaneously occupied by LY341495 and CDPPB are distinct from those sampled by CDPPB alone, or CDPPB with a small population occupied by the low ambient glutamate levels.

Probe dependence is operative at $mGlu_5$, manifesting as differences in the magnitude of cooperativity depending on the orthosteric agonist used (Hellyer et al., 2020; Sengmany et al., 2017). Probe dependent PAMs include DPFE (structurally related to compound 2c) and acetylenic PAMs (which share an overlapping pharmacophore with MPPA). Herein, CDPPB did not show probe dependence; affinity and cooperativity estimates derived from interactions with either DHPG or L-glutamate were similar, consistent with our earlier report (Sengmany et al., 2017). Further, affinity and cooperativity estimates for MPPA and compound 2c determined from potentiation curves of DHPG or L-glutamate were also similar, despite belonging to structural classes of $mGlu_5$ PAMs that show probe dependence. These findings build on the evidence base that structurally similar $mGlu_5$ allosteric ligands can differentially exhibit probe dependence, representing an important consideration when interpreting structure-activity relationships within a discovery program.

Molecular Pharmacology Fast Forward. Published on February 18, 2021 as DOI: 10.1124/molpharm.120.000185
This article has not been copyedited and formatted. The final version may differ from this version.

Related to probe dependence is the idea that allosteric modulators can engender biased modulation, as evidenced by different magnitudes of affinity or cooperativity depending on the measure of receptor activity in the presence of the same orthosteric agonist. For $mGlu_5$, biased modulation has been observed for allosteric ligands classified as NAMs or PAMs based on Ca^{2+} mobilization assays (Arsova et al., 2020; Sengmany et al., 2019; Sengmany et al., 2017). Here we show that MPPA is a biased $mGlu_5$ PAM, where the magnitude of cooperativity with orthosteric agonists is lower/neutral when measured in IP_1 accumulation or receptor internalization when compared with Ca^{2+} mobilization and ERK1/2 phosphorylation in HEK293A-$mGlu_5$ cells. These data are in agreement with previous reports for $mGlu_5$ where cooperativity was lower when measured in IP_1 accumulation assays over Ca^{2+} mobilization (Sengmany et al., 2019; Sengmany et al., 2017). Although $mGlu_5$ couples predominantly to $G_{q/11}$ proteins to elevate IP_3 levels and release of Ca^{2+} from intracellular stores, $mGlu_5$ also couples to G_s and modulates the activity of multiple ion channels (enabling extracellular Ca^{2+} influx) in a $G_{q/11}$-independent fashion (reviewed in (Gregory and Goudet, 2021)). Both intracellular release and extracellular influx of Ca^{2+} were measured in the assays used herein. Therefore, the biased agonism and modulation observed for $mGlu_5$ PAMs between two measures that are traditionally considered linked likely arises due to stabilizing receptor conformations that differentially favor these different effectors. A key difference between the responses where MPPA cooperativity is greater is the temporal nature of the assays. Ca^{2+} mobilization and ERK1/2 phosphorylation are short-lived in comparison to IP_1 accumulation and receptor internalization, which are both measured over 1 hour. Measuring a non-equilibrium response can influence how signaling bias is observed, as previously shown for the dopamine D_2 receptor (Klein Herenbrink et al., 2016). In contrast, compound 2c cooperativity estimates with DHPG and L-glutamate were not significantly different across all

Molecular Pharmacology Fast Forward. Published on February 18, 2021 as DOI: 10.1124/molpharm.120.000185
This article has not been copyedited and formatted. The final version may differ from this version.

measures. However, the intrinsic efficacy of CDPPB or high positive cooperativity of compound 2c prohibited quantification of these parameters in certain assays using the modulator titration paradigm employed here. Importantly, biased cooperativity of MPPA with DHPG between IP_1 accumulation and Ca^{2+} mobilization translated to natively expressed $mGlu_5$. The observation that magnitudes of cooperativity can differ depending on the measure of receptor activity may contribute to the challenges in translating *in vitro* profiles to efficacy *in vivo*, particularly in discovery pipelines where cooperativity is determined from a single measure.

Context and cell background are important considerations when classifying $mGlu_5$ ligand pharmacology. Pharmacological profiles in primary cortical neurons differed to recombinant cells. In primary cortical neurons, none of the three ligands showed intrinsic efficacy for Ca^{2+} mobilization and all were robust partial agonists for IP_1 accumulation. For select $mGlu_5$ PAMs, agonist activity for Ca^{2+} mobilization has been linked to receptor expression levels in recombinant cells and is not always recapitulated in native cells (Noetzel et al., 2012). The biased agonism profiles for $mGlu_5$ PAM-agonists can be different between recombinant and native systems as well (Sengmany et al., 2017). In native systems, $mGlu_5$ forms oligomeric complexes with: 1) other GPCRs, 2) surface proteins and 3) scaffolding proteins via the C-tail (Pin and Bettler, 2016); differing complements of effectors, regulatory and scaffolding proteins have the capacity to shape $mGlu_5$ signaling in a cell-type dependent manner. In addition, $mGlu_5$ is found on intracellular membranes, such that the cellular response to $mGlu_5$ activation may differ depending on where it is generated from and accessibility of ligands to different subcellular compartments (Jong et al., 2019; Jong et al., 2014). Recombinant versus native cells may have different ambient glutamate levels or glutamate may be released in an activity dependent manner. All of these factors may contribute to the mechanisms underlying

Molecular Pharmacology Fast Forward. Published on February 18, 2021 as DOI: 10.1124/molpharm.120.000185
This article has not been copyedited and formatted. The final version may differ from this version.

biased $mGlu_5$ modulation. Future experiments could employ selective inhibitors of co-expressed channels and transporters to decipher these underlying mechanisms.

Compound 2c consistently had the greatest degree of positive cooperativity, independent of the orthosteric ligand or response measured. While compound 2c has not yet been tested for *in vivo* efficacy, related compounds have demonstrated anti-psychotic efficacy and pro-cognitive effects in preclinical models (Gregory et al., 2013; Xiong et al., 2010). The magnitude of $mGlu_5$ PAM cooperativity with L-glutamate based on Ca^{2+} mobilization was recently shown to correlate with efficacy in the amphetamine hyperlocomotion assay (Gregory et al., 2019). However, whether such correlations extend to structurally diverse $mGlu_5$ PAMs remains to be tested. Indeed, MPPA has higher positive cooperativity than CDPPB, yet a lower CDPPB dose is required for efficacy in reducing amphetamine-induced hyperlocomotion in rats relative to MPPA (Kinney et al., 2005; Sharma et al., 2009). It is unknown how the pharmacokinetics of MPPA compares with CDPPB. Additionally, differences in receptor residency times may also be linked to *in vivo* efficacy; further investigation is warranted.

In summary, we have determined the binding and signaling profiles of three $mGlu_5$ PAMs from distinct scaffolds at four measures of $mGlu_5$ function in recombinant cells. Key differences in *in vitro* pharmacological profiles translated to natively expressed $mGlu_5$ in primary cortical neurons. By assessing the kinetics of PAM binding to the $mGlu_5$ receptor, we reveal previously unappreciated differences that may contribute to observations of PAM agonist activity, as well as biased cooperativity. Improved molecular characterization provides a better basis to understand the pharmacological properties of $mGlu_5$ PAMs, which can be implemented in the future for improved structure-activity relationship interrogation and rational drug discovery.

Molecular Pharmacology Fast Forward. Published on February 18, 2021 as DOI: 10.1124/molpharm.120.000185
This article has not been copyedited and formatted. The final version may differ from this version.

Acknowledgements

We thank Drs. Morten Jørgensen and Søren Møller Nielsen, H. Lundbeck A/S for providing the PAMs tested in this study.

Molecular Pharmacology Fast Forward. Published on February 18, 2021 as DOI: 10.1124/molpharm.120.000185
This article has not been copyedited and formatted. The final version may differ from this version.

Authorship Contributions

Participated in research design: Arsova, Vedel, Hansen, Foster, Bräuner-Osborne, Gregory

Conducted experiments: Arsova, Møller, Hellyer, Gregory

Performed data analysis: Arsova, Møller, Hellyer, Gregory

Wrote or contributed to drafting the manuscript: Arsova, Møller, Bräuner-Osborne, Gregory

Editing and approval of final manuscript: All authors

Molecular Pharmacology Fast Forward. Published on February 18, 2021 as DOI: 10.1124/molpharm.120.000185
This article has not been copyedited and formatted. The final version may differ from this version.

References

Arsova A, Møller TC, Vedel L, Hansen JL, Foster SR, Gregory KJ and Bräuner-Osborne H (2020) Detailed In Vitro Pharmacological Characterization of Clinically Tested Negative Allosteric Modulators of the Metabotropic Glutamate Receptor 5. *Mol Pharmacol* **98**(1): 49-60.

Black JW, Leff P, Shankley NP and Wood J (1985) An operational model of pharmacological agonism: the effect of E/[A] curve shape on agonist dissociation constant estimation. *Br J Pharmacol* **84**(2): 561-571.

Brabet I, Parmentier ML, De Colle C, Bockaert J, Acher F and Pin JP (1998) Comparative effect of L-CCG-I, DCG-IV and gamma-carboxy-L-glutamate on all cloned metabotropic glutamate receptor subtypes. *Neuropharmacology* **37**(8): 1043-1051.

Bridges TM, Rook JM, Noetzel MJ, Morrison RD, Zhou Y, Gogliotti RD, Vinson PN, Xiang Z, Jones CK, Niswender CM, Lindsley CW, Stauffer SR, Conn PJ and Daniels JS (2013) Biotransformation of a novel positive allosteric modulator of metabotropic glutamate receptor subtype 5 contributes to seizure-like adverse events in rats involving a receptor agonism-dependent mechanism. *Drug Metab Dispos* **41**(9): 1703-1714.

Changeux JP and Christopoulos A (2017) Allosteric modulation as a unifying mechanism for receptor function and regulation. *Diabetes Obes Metab* **19 Suppl 1**: 4-21.

Chen Y, Nong Y, Goudet C, Hemstapat K, de Paulis T, Pin JP and Conn PJ (2007) Interaction of novel positive allosteric modulators of metabotropic glutamate receptor 5 with the negative allosteric antagonist site is required for potentiation of receptor responses. *Mol Pharmacol* **71**(5): 1389-1398.

Christopher JA, Orgovan Z, Congreve M, Dore AS, Errey JC, Marshall FH, Mason JS, Okrasa K, Rucktooa P, Serrano-Vega MJ, Ferenczy GG and Keseru GM (2018) Structure-

Based Optimization Strategies for G Protein-Coupled Receptor (GPCR) Allosteric Modulators: A Case Study from Analyses of New Metabotropic Glutamate Receptor 5 (mGlu5) X-ray Structures. *J Med Chem*.

Copeland RA (2016) The drug-target residence time model: a 10-year retrospective. *Nat Rev Drug Discov* **15**(2): 87-95.

Dhami GK and Ferguson SS (2006) Regulation of metabotropic glutamate receptor signaling, desensitization and endocytosis. *Pharmacol Ther* **111**(1): 260-271.

Doornbos MLJ, Cid JM, Haubrich J, Nunes A, van de Sande JW, Vermond SC, Mulder-Krieger T, Trabanco AA, Ahnaou A, Drinkenburg WH, Lavreysen H, Heitman LH, AP IJ and Tresadern G (2017) Discovery and Kinetic Profiling of 7-Aryl-1,2,4-triazolo[4,3-a]pyridines: Positive Allosteric Modulators of the Metabotropic Glutamate Receptor 2. *J Med Chem* **60**(15): 6704-6720.

Dore AS, Okrasa K, Patel JC, Serrano-Vega M, Bennett K, Cooke RM, Errey JC, Jazayeri A, Khan S, Tehan B, Weir M, Wiggin GR and Marshall FH (2014) Structure of class C GPCR metabotropic glutamate receptor 5 transmembrane domain. *Nature* **511**(7511): 557-562.

Doumazane E, Scholler P, Zwier JM, Trinquet E, Rondard P and Pin JP (2011) A new approach to analyze cell surface protein complexes reveals specific heterodimeric metabotropic glutamate receptors. *FASEB J* **25**(1): 66-77.

Ferguson SSG (2001) Evolving concepts in G protein-coupled receptor endocytosis: The role in receptor desensitization and signaling. *Pharmac Rev* **53**(1).

Foster DJ and Conn PJ (2017) Allosteric Modulation of GPCRs: New Insights and Potential Utility for Treatment of Schizophrenia and Other CNS Disorders. *Neuron* **94**(3): 431-446.

Foster SR and Bräuner-Osborne H (2018) Investigating internalization and intracellular trafficking of GPCRs: New techniques and real-time experimental approaches. *Handb Exp Pharmacol* **245**: 41-61.

Gentry PR, Sexton PM and Christopoulos A (2015) Novel Allosteric Modulators of G Protein-coupled Receptors. *J Biol Chem* **290**(32): 19478-19488.

Gregory KJ, Bridges TM, Gogliotti RG, Stauffer SR, Noetzel MJ, Jones CK, Lindsley CW, Conn PJ and Niswender CM (2019) In Vitro to in Vivo Translation of Allosteric Modulator Concentration-Effect Relationships: Implications for Drug Discovery. *ACS Pharmacol Transl Sci* **2**(6): 442-452.

Gregory KJ and Goudet C (2021) International Union of Basic and Clinical Pharmacology. CXI. Pharmacology, Signaling, and Physiology of Metabotropic Glutamate Receptors. *Pharmacol Rev* **73**(1): 521-569.

Gregory KJ, Herman EJ, Ramsey AJ, Hammond AS, Byun NE, Stauffer SR, Manka JT, Jadhav S, Bridges TM, Weaver CD, Niswender CM, Steckler T, Drinkenburg WH, Ahnaou A, Lavreysen H, Macdonald GJ, Bartolome JM, Mackie C, Hrupka BJ, Caron MG, Daigle TL, Lindsley CW, Conn PJ and Jones CK (2013) N-aryl piperazine metabotropic glutamate receptor 5 positive allosteric modulators possess efficacy in preclinical models of NMDA hypofunction and cognitive enhancement. *J Pharmacol Exp Ther* **347**(2): 438-457.

Gregory KJ, Noetzel MJ, Rook JM, Vinson PN, Stauffer SR, Rodriguez AL, Emmitte KA, Zhou Y, Chun AC, Felts AS, Chauder BA, Lindsley CW, Niswender CM and Conn PJ (2012) Investigating metabotropic glutamate receptor 5 allosteric modulator cooperativity, affinity, and agonism: enriching structure-function studies and structure-activity relationships. *Mol Pharmacol* **82**(5): 860-875.

Guo D, Hillger JM, AP IJ and Heitman LH (2014) Drug-target residence time--a case for G protein-coupled receptors. *Med Res Rev* **34**(4): 856-892.

Hellyer SD, Albold S, Sengmany K, Singh J, Leach K and Gregory KJ (2019) Metabotropic glutamate receptor 5 (mGlu5)-positive allosteric modulators differentially induce or potentiate desensitization of mGlu5 signaling in recombinant cells and neurons. *J Neurochem* **151**(3): 301-315.

Hellyer SD, Albold S, Wang T, Chen AN, May LT, Leach K and Gregory KJ (2018) "Selective" Class C G protein-coupled receptor modulators are neutral or biased mGlu5 allosteric ligands. *Mol Pharmacol*.

Hellyer SD, Sengmany K, Keller AN, Christopoulos A, Leach K and Gregory KJ (2020) Probe dependence and biased potentiation of metabotropic glutamate receptor 5 is mediated by differential ligand interactions in the common allosteric binding site. *Biochem Pharmacol* **177**: 114013.

Horio M, Fujita Y and Hashimoto K (2013) Therapeutic effects of metabotropic glutamate receptor 5 positive allosteric modulator CDPPB on phencyclidine-induced cognitive deficits in mice. *Fundam Clin Pharmacol* **27**(5): 483-488.

Ito I, Kohda A, Tanabe S, Hirose E, Hayashi M, Mitsunaga S and Sugiyama H (1992) 3,5-Dihydroxyphenyl-glycine: a potent agonist of metabotropic glutamate receptors. *Neuroreport* **3**(11): 1013-1016.

Jong YI, Harmon SK and O'Malley KL (2019) Location and Cell-Type-Specific Bias of Metabotropic Glutamate Receptor, mGlu5, Negative Allosteric Modulators. *ACS Chem Neurosci* **10**(11): 4558-4570.

Jong YJ, Sergin I, Purgert CA and O'Malley KL (2014) Location-dependent signaling of the group 1 metabotropic glutamate receptor mGlu5. *Mol Pharmacol* **86**(6): 774-785.

Kapur S and Seeman P (2001) Does fast dissociation from the dopamine d(2) receptor explain the action of atypical antipsychotics?: A new hypothesis. *Am J Psychiatry* **158**(3): 360-369.

Kenakin T and Christopoulos A (2013) Signalling bias in new drug discovery: detection, quantification and therapeutic impact. *Nat Rev Drug Discov* **12**(3): 205-216.

Kingston AE, Ornstein PL, Wright RA, Johnson BG, Mayne NG, Burnett JP, Belagaje R, Wu S and Schoepp DD (1998) LY341495 is a nanomolar potent and selective antagonist of group II metabotropic glutamate receptors. *Neuropharmacology* **37**(1): 1-12.

Kinney GG, O'Brien JA, Lemaire W, Burno M, Bickel DJ, Clements MK, Chen TB, Wisnoski DD, Lindsley CW, Tiller PR, Smith S, Jacobson MA, Sur C, Duggan ME, Pettibone DJ, Conn PJ and Williams DL, Jr. (2005) A novel selective positive allosteric modulator of metabotropic glutamate receptor subtype 5 has in vivo activity and antipsychotic-like effects in rat behavioral models. *J Pharmacol Exp Ther* **313**(1): 199-206.

Klein Herenbrink C, Sykes DA, Donthamsetti P, Canals M, Coudrat T, Shonberg J, Scammells PJ, Capuano B, Sexton PM, Charlton SJ, Javitch JA, Christopoulos A and Lane JR (2016) The role of kinetic context in apparent biased agonism at GPCRs. *Nat Commun* **7**: 10842.

Lane JR, May LT, Parton RG, Sexton PM and Christopoulos A (2017) A kinetic view of GPCR allostery and biased agonism. *Nat Chem Biol* **13**(9): 929-937.

Levoye A, Zwier JM, Jaracz-Ros A, Klipfel L, Cottet M, Maurel D, Bdioui S, Balabanian K, Prézeau L, Trinquet E, Durroux T and Bachelerie F (2015) A Broad G Protein-Coupled Receptor Internalization Assay that Combines SNAP-Tag Labeling, Diffusion-Enhanced

Resonance Energy Transfer, and a Highly Emissive Terbium Cryptate. *Front Endocrinol (Lausanne)* **6**: 167.

Lindstrom E, von Mentzer B, Pahlman I, Ahlstedt I, Uvebrant A, Kristensson E, Martinsson R, Noven A, de Verdier J and Vauquelin G (2007) Neurokinin 1 receptor antagonists: correlation between in vitro receptor interaction and in vivo efficacy. *J Pharmacol Exp Ther* **322**(3): 1286-1293.

Melancon BJ, Hopkins CR, Wood MR, Emmitte KA, Niswender CM, Christopoulos A, Conn PJ and Lindsley CW (2012) Allosteric modulation of seven transmembrane spanning receptors: theory, practice, and opportunities for central nervous system drug discovery. *J Med Chem* **55**(4): 1445-1464.

Motulsky HJ and Mahan LC (1984) The kinetics of competitive radioligand binding predicted by the law of mass action. *Mol Pharmacol* **25**(1): 1-9.

Mutel V, Ellis GJ, Adam G, Chaboz S, Nilly A, Messer J, Bleuel Z, Metzler V, Malherbe P, Schlaeger EJ, Roughley BS, Faull RL and Richards JG (2000) Characterization of [(3)H]Quisqualate binding to recombinant rat metabotropic glutamate 1a and 5a receptors and to rat and human brain sections. *J Neurochem* **75**(6): 2590-2601.

Nicoletti F, Bruno V, Ngomba RT, Gradini R and Battaglia G (2015) Metabotropic glutamate receptors as drug targets: what's new? *Curr Opin Pharmacol* **20**: 89-94.

Noetzel MJ, Rook JM, Vinson PN, Cho HP, Days E, Zhou Y, Rodriguez AL, Lavreysen H, Stauffer SR, Niswender CM, Xiang Z, Daniels JS, Jones CK, Lindsley CW, Weaver CD and Conn PJ (2012) Functional impact of allosteric agonist activity of selective positive allosteric modulators of metabotropic glutamate receptor subtype 5 in regulating central nervous system function. *Mol Pharmacol* **81**(2): 120-133.

Parmentier-Batteur S, Hutson PH, Menzel K, Uslaner JM, Mattson BA, O'Brien JA, Magliaro BC, Forest T, Stump CA, Tynebor RM, Anthony NJ, Tucker TJ, Zhang XF, Gomez R, Huszar SL, Lambeng N, Faure H, Le Poul E, Poli S, Rosahl TW, Rocher JP, Hargreaves R and Williams TM (2014) Mechanism based neurotoxicity of mGlu5 positive allosteric modulators--development challenges for a promising novel antipsychotic target. *Neuropharmacology* **82**: 161-173.

Parmentier-Batteur S, O'Brien JA, Doran S, Nguyen SJ, Flick RB, Uslaner JM, Chen H, Finger EN, Williams TM, Jacobson MA and Hutson PH (2012) Differential effects of the mGluR5 positive allosteric modulator CDPPB in the cortex and striatum following repeated administration. *Neuropharmacology* **62**(3): 1453-1460.

Pedersen MF, Wrobel TM, Marcher-Rorsted E, Pedersen DS, Møller TC, Gabriele F, Pedersen H, Matosiuk D, Foster SR, Bouvier M and Bräuner-Osborne H (2020) Biased agonism of clinically approved mu-opioid receptor agonists and TRV130 is not controlled by binding and signaling kinetics. *Neuropharmacology* **166**: 107718.

Pin JP and Bettler B (2016) Organization and functions of mGlu and $GABA_B$ receptor complexes. *Nature* **540**(7631): 60-68.

Roed SN, Wismann P, Underwood CR, Kulahin N, Iversen H, Cappelen KA, Schaffer L, Lehtonen J, Hecksher-Soerensen J, Secher A, Mathiesen JM, Bräuner-Osborne H, Whistler JL, Knudsen SM and Waldhoer M (2014) Real-time trafficking and signaling of the glucagon-like peptide-1 receptor. *Mol Cell Endocrinol* **382**(2): 938-949.

Rook JM, Noetzel MJ, Pouliot WA, Bridges TM, Vinson PN, Cho HP, Zhou Y, Gogliotti RD, Manka JT, Gregory KJ, Stauffer SR, Dudek FE, Xiang Z, Niswender CM, Daniels JS, Jones CK, Lindsley CW and Conn PJ (2013) Unique signaling profiles of positive

allosteric modulators of metabotropic glutamate receptor subtype 5 determine differences in in vivo activity. *Biol Psychiatry* **73**(6): 501-509.

Sengmany K, Hellyer SD, Albold S, Wang T, Conn PJ, May LT, Christopoulos A, Leach K and Gregory KJ (2019) Kinetic and system bias as drivers of metabotropic glutamate receptor 5 allosteric modulator pharmacology. *Neuropharmacology* **149**: 83-96.

Sengmany K, Singh J, Stewart GD, Conn PJ, Christopoulos A and Gregory KJ (2017) Biased allosteric agonism and modulation of metabotropic glutamate receptor 5: Implications for optimizing preclinical neuroscience drug discovery. *Neuropharmacology* **115**: 60-72.

Sharma S, Kedrowski J, Rook JM, Smith RL, Jones CK, Rodriguez AL, Conn PJ and Lindsley CW (2009) Discovery of molecular switches that modulate modes of metabotropic glutamate receptor subtype 5 (mGlu5) pharmacology in vitro and in vivo within a series of functionalized, regioisomeric 2- and 5-(phenylethynyl)pyrimidines. *J Med Chem* **52**(14): 4103-4106.

Smith JS, Lefkowitz RJ and Rajagopal S (2018) Biased signalling: from simple switches to allosteric microprocessors. *Nat Rev Drug Discov*.

Trinh PNH, May LT, Leach K and Gregory KJ (2018) Biased agonism and allosteric modulation of metabotropic glutamate receptor 5. *Clin Sci (Lond)* **132**(21): 2323-2338.

Tummino PJ and Copeland RA (2008) Residence time of receptor-ligand complexes and its effect on biological function. *Biochemistry* **47**(20): 5481-5492.

Unett DJ, Gatlin J, Anthony TL, Buzard DJ, Chang S, Chen C, Chen X, Dang HT, Frazer J, Le MK, Sadeque AJ, Xing C and Gaidarov I (2013) Kinetics of 5-HT2B receptor signaling: profound agonist-dependent effects on signaling onset and duration. *J Pharmacol Exp Ther* **347**(3): 645-659.

Valenti O, Conn PJ and Marino MJ (2002) Distinct physiological roles of the Gq-coupled metabotropic glutamate receptors Co-expressed in the same neuronal populations. *J Cell Physiol* **191**(2): 125-137.

Vauquelin G and Charlton SJ (2010) Long-lasting target binding and rebinding as mechanisms to prolong in vivo drug action. *Br J Pharmacol* **161**(3): 488-508.

Waung MW and Huber KM (2009) Protein translation in synaptic plasticity: mGluR-LTD, Fragile X. *Curr Opin Neurobiol* **19**(3): 319-326.

Wellendorph P and Bräuner-Osborne H (2009) Molecular basis for amino acid sensing by family C G-protein-coupled receptors. *Br J Pharmacol* **156**(6): 869-884.

Xiong H, Brugel TA, Balestra M, Brown DG, Brush KA, Hightower C, Hinkley L, Hoesch V, Kang J, Koether GM, McCauley JP, Jr., McLaren FM, Panko LM, Simpson TR, Smith RW, Woods JM, Brockel B, Chhajlani V, Gadient RA, Spear N, Sygowski LA, Zhang M, Arora J, Breysse N, Wilson JM, Isaac M, Slassi A and King MM (2010) 4-aryl piperazine and piperidine amides as novel mGluR5 positive allosteric modulators. *Bioorg Med Chem Lett* **20**(24): 7381-7384.

Molecular Pharmacology Fast Forward. Published on February 18, 2021 as DOI: 10.1124/molpharm.120.000185
This article has not been copyedited and formatted. The final version may differ from this version.

Footnotes

a) Financial support

A. A. acknowledges financial support from the University of Copenhagen, Oticon Foundation, and Torben and Alice Frimodts Foundation. H.B.-O. acknowledges financial support from the Augustinus Foundation, the Lundbeck Foundation and the Independent Research Fund Denmark. This project received funding from the European Union's Horizon 2020 research and innovation program under the Marie Sklodowska-Curie grant agreement No 797497 (T.C.M.). S.R.F. acknowledges financial support from the Lundbeck Foundation and the Independent Research Fund Denmark. This work was supported by the National Health & Medical Research Council of Australia (NHMRC): Project Grants APP1084775 (K.J.G.) and APP1127322 (K.J.G.). K.J.G. is supported by an Australian Research Council Future Fellowship: FT170100392. J.L.H. was an employee and shareholder of Novo Nordisk A/S at the time of the study. There are no conflicts of interest to declare.

b) Unnumbered footnote

A prior version of the paper was included in the PhD thesis: Arsova A (2018) Biased signaling and allosteric modulation of metabotropic glutamate receptor 5. Faculty of Health and Medical Sciences, University of Copenhagen, Copenhagen, Denmark.

c) To whom requests for reprints should be addressed:

Name: Karen J. Gregory

Address: 381 Royal Parade, Parkville, VIC, Australia, 3052

Telephone: +61 399039243

Email: karen.gregory@monash.edu

d) Numbered footnotes

[1]*A.A. and T.C.M. contributed equally to this work.*

Molecular Pharmacology Fast Forward. Published on February 18, 2021 as DOI: 10.1124/molpharm.120.000185
This article has not been copyedited and formatted. The final version may differ from this version.

[2]*H.B-O. and K.J.G. contributed equally to this work.*

Molecular Pharmacology Fast Forward. Published on February 18, 2021 as DOI: 10.1124/molpharm.120.000185
This article has not been copyedited and formatted. The final version may differ from this version.

Figure legends

Fig. 1. Inhibition of [^{3}H]methoxy-PEPy binding using HEK293A-mGlu$_5$-low cell membranes. Displacement by each of the three PAMs was measured after 1 h incubation at room temperature. Data was normalized to 0 as 0% and to 100% as the mean for the total specific binding. Data points represent mean + SD (duplicate measurement) from 4 (MPPA and CDPPB) or 6 (compound 2c) independent experiments. For compound 2c, the displacement curve was fitted equally well with a competitive (dashed line) versus allosteric (solid line) model.

Fig. 2. Kinetics of binding with HEK293A-mGlu$_5$-low cell membranes. Competition association binding with [^{3}H]methoxy-PEPy and indicated concentrations of each PAM. Data represented as mean + SD (duplicate measurements) from 6 (MPPA), 4 (CDPPB competition experiments), 8 (CDPPB vehicle experiments), or 3 (compound 2c) independent experiments.

Fig. 3. Intrinsic PAM-agonist activity in HEK293A-mGlu$_5$-low cells. (A) Peak Ca^{2+} mobilization measurement measured 90 s after PAM or DHPG addition at 37°C, expressed as % maximal DHPG response. (B) IP_1 accumulation measured 1 h after PAM or DHPG addition at 37°C, expressed as % maximal DHPG response. (C) ERK1/2 phosphorylation measurement after 5 min incubation of PAM or DHPG addition at 37°C. In the presence of 300 µM LY341495, the response to PAMs or DHPG is diminished for Ca^{2+} mobilization (D), IP_1 accumulation (E) or ERK1/2 phosphorylation (F). Data in panels D-F are expressed as a % maximal DHPG response in the absence of LY341495, where 0% is defined by vehicle treated in the presence of LY341495. The effect of LY341495 on basal responses in each

Molecular Pharmacology Fast Forward. Published on February 18, 2021 as DOI: 10.1124/molpharm.120.000185
This article has not been copyedited and formatted. The final version may differ from this version.

assay is shown in Supplemental Fig 1. Dashed line in panels D-F shows the response to DHPG concentration-response relationship (from panels A-C) in the absence of LY341495 for reference. Data are mean + SD (duplicate measurements) from 3-11 independent experiments (refer to Table 2 for exact numbers).

Fig. 4. Potentiation of orthosteric agonist responses in HEK293A-mGlu$_5$-low cells. Ca^{2+} mobilization after stimulation with orthosteric agonist alone or simultaneous addition of PAM and 100 nM L-glutamate (A) or DHPG (B). IP_1 accumulation in response to incubation with orthosteric agonist alone or co-incubation with PAM and 1 µM L-glutamate (C) or DHPG (D). Phosphorylated ERK1/2 levels after stimulation with orthosteric agonist alone or simultaneous addition of PAMs and 500 nM L-glutamate (E) or DHPG (F). Data points are mean + SD (triplicate measurements) from 3-6 independent experiments (refer to Table 3 and Supplemental Table 1 for exact numbers). Data were normalized to buffer as 0% and to the maximal L-glutamate (A, C), maximal DHPG (B, D) or 10% FBS (E, F) responses as 100%.

Fig. 5. Real-time measurement of mGlu$_5$ internalization. HEK293A cells were transiently transfected with HA-SNAP-mGlu$_5$ and EAAT3 (HEK293A-SNAP-mGlu$_5$), and internalization measured as a change in fluorescence over time. (A-C) Indicated concentrations of each PAM were added at t = 0 min and surface mGlu$_5$ levels tracked for 66 min. (D-F) PAM-induced mGlu$_5$ internalization in the presence of 300 µM LY341495. (G-I) Potentiation of L-glutamate-induced mGlu$_5$ internalization by indicated PAMs. The L-glutamate concentration was increased by partially blocking the EAAT3 glutamate transporter with 30 µM DL-TBOA. (J-L) Potentiation of 1 µM DHPG-induced mGlu$_5$ internalization by indicated PAMs. Data points are mean + SD (triplicate measurements) from 3 independent

Molecular Pharmacology Fast Forward. Published on February 18, 2021 as DOI: 10.1124/molpharm.120.000185
This article has not been copyedited and formatted. The final version may differ from this version.

experiments and solid lines are nonlinear regression fit to an exponential model of one-phase association.

Fig. 6. Concentration-response relationships for agonism and potentiation of $mGlu_5$ internalization. From the kinetic measurements in Fig. 5, the area under the curve was calculated for each ligand concentration and normalized to the maximal orthosteric agonist response measured in parallel. Each PAM was tested alone (A) and in the presence of 300 µM LY341495 (B). Each PAM was assessed for potentiation of L-glutamate (by partially blocking L-glutamate transport with 30 µM DL-TBOA) (C) or 1 µM DHPG (D) induced $mGlu_5$ internalization. Data are mean + SD (triplicate measurement) from 3 or 4 (L-glutamate) independent experiments. For reference, the control curve for DHPG (without LY341495) is shown by the dashed line in B. Error bars not shown lie within the dimensions of the symbol.

Fig. 7. Assessment of biased agonism or modulation in HEK293A-$mGlu_5$-low or HEK293A-SNAP-$mGlu_5$ cells. (A) For CDPPB intrinsic agonism, $\Delta\log(\tau/K_A)$ values (relative to DHPG) were derived from concentration-response curves in the presence of LY341495. (B) Cooperativity factors for each functional response are presented relative to the value calculated from Ca^{2+} mobilization. Cooperativity with DHPG is depicted in squares. Cooperativity with L-glutamate is depicted in triangles. For select PAMs and functional outputs, cooperativity could not be determined (n.a.) or was indistinguishable from neutral due to intrinsic PAM-agonist activity. Data are mean and 95% CI from 3-5 independent experiments (refer to Tables 2 and 4 for exact numbers). $*P < 0.05$, one-way ANOVA with Tukey's multiple comparisons test.

Molecular Pharmacology Fast Forward. Published on February 18, 2021 as DOI: 10.1124/molpharm.120.000185
This article has not been copyedited and formatted. The final version may differ from this version.

Fig. 8. PAM agonism and potentiation of DHPG in cortical neurons. Intrinsic agonist activity of PAMs in primary cortical neurons for Ca^{2+} mobilization (A) and IP_1 accumulation (B). (C) PAM potentiation of 120 nM DHPG was assessed in Ca^{2+} mobilization assays with simultaneous addition. (D) For IP_1 accumulation PAM potentiation was assessed in the presence of 1 μM DHPG, since DHPG has lower potency in this assay. Data are mean + SD (duplicate measurements) from 4-9 independent experiments (refer to Table 5 for exact numbers). Data were normalized to 0% as buffer and 100% maximal DHPG response.

Tables

Table 1

Affinity and kinetics of binding estimates for $mGlu_5$ PAMs obtained from competition binding experiments with [^{3}H]methoxy-PEPy in HEK293A-$mGlu_5$-low cells. Data represent the mean and 95% CI of *n* independent experiments performed in duplicate.

	Equilibrium radioligand displacement				**Competition association binding**				
Ligand	pK_I[a] *(95% CI)*	pK_B[b] *(95% CI)*	$log\alpha$[c] *(95% CI*	*n*	k_{on} [$\times10^6$ ($M^{-1}min^{-1}$)][d] *(95% CI)*	k_{off} (min^{-1})[e] *(95% CI)*	*RT (min)*[f]	pK_D[g]	*n*
MPPA	6.51 (6.25 - 6.77)	n.d.	n.d.	4	11.0 (3.7 - 18.2)	1	n.d.	n.d.	6
CDPPB	n.d.	7.27 (6.79 - 7.74)	-0.64 (-1.10 - -0.24)	4	1.91 (-0.3 - 4.1)	0.211 (0.067 - 0.356)	4.7	6.96	6
compound 2c	5.17 (5.08 - 5.27)[h]	5.36 (5.19 - 5.53)	-0.96 (-1.17 - -0.75)	6	0.16 (-0.01 - 0.34)	1	n.d.	n.d.	3

n.d. not determined due to no fit with the given model.

[a]Negative logarithm of the equilibrium dissociation constant determined with a competitive binding model.

[b]Negative logarithm of the equilibrium dissociation constant determined with an allosteric binding model.

[c]Logarithm of the cooperativity factor.

[d]Association rate constant.

[e]Dissociation rate constant. For ligands with fast k_{off}, global analyses could not derive k_{off}, therefore the value was constrained to 1, to enable estimation of $k_{on.}$

[f]RT, residence time defined as $1/k_{off}$.

[g]Negative logarithm of the equilibrium dissociation constant determined from kinetic parameters (k_{off}/k_{on}).

[h]Assumed full displacement (= constrained minimum to 0%).

Table 2

Affinity (pK_A) and $\log(\tau/K_A)$ estimates for the agonist activity of DHPG or $mGlu_5$ PAMs in HEK293A-$mGlu_5$-low or HEK293A-SNAP-$mGlu_5$ cells. Estimates were derived in the presence of the orthosteric antagonist LY341495 to ensure that only the intrinsic agonist activity of the PAMs was measured. Data represent the mean and 95% CI of *n* independent experiments performed in duplicate or triplicate (internalization assay).

	Ca^{2+} mobilization			**IP_1 accumulation**			**pERK1/2**			**Internalization**		
Ligand	*pK_A[a] (95% CI)*	*$\log(\tau/K_A)$[b] (95% CI)*	*n*	*pK_A (95% CI)*	*$\log(\tau/K_A)$ (95% CI)*	*n*	*pK_A (95% CI)*	*$\log(\tau/K_A)$ (95% CI)*	*n*	*pK_A (95% CI)*	*$\log(\tau/K_A)$ (95% CI)*	*n*
DHPG	n.d.	6.78 (6.64 - 6.93)	3	n.d.	5.89 (5.80 - 5.98)	5	n.d.	6.06 (5.99 - 6.13)	11	n.d.	5.43 (5.36 - 5.50)	3
MPPA	n.r.	n.r.	4	n.r.	n.r.	3	n.r.	n.r.	3	n.r.	n.r.	3
CDPPB	7.20 (6.36 - 7.94)	6.71 (5.88 - 7.55)	4	n.d.	6.18 (5.89 - 6.47)	5	7.14 (6.58 - 7.61)	7.03 (6.56 - 7.58)	5	5.57 (5.22 - 5.96)[c]	5.55 (5.29 - 5.83)	3
compound 2c	n.r.	n.r.	4	n.r.	n.r.	3	n.r.	n.r.	3	n.r.	n.r.	3

n.d. not determined; n.r. no response.

[a]pK_A, negative logarithm of the equilibrium dissociation binding constant determined with the operational model of agonism.

[b]$\log(\tau/K_A)$, transduction coefficient; τ, intrinsic efficacy.

[c]$P < 0.05$ when compared with estimates from Ca^{2+} mobilization or IP_1 accumulation by one-way ANOVA with Tukey's multiple comparisons test.

Table 3

Affinity estimates for allosteric modulation of low concentrations of orthosteric ligand (L-glutamate or DHPG) in HEK293A-mGlu$_5$-low or HEK293A-SNAP-mGlu$_5$ cells. Data represent the mean and 95% CI of *n* independent experiments performed in triplicate.

	Ca^{2+} mobilization		**IP_1 accumulation**		**pERK1/2**		**Internalization[a]**	
Ligand	*pK_B[b] (95% CI)*	*n*	*pK_B (95% CI)*	*n*	*pK_B (95% CI)*	*n*	*pK_B (95% CI)*	*n*
L-glutamate								
MPPA	7.11 (6.70 - 7.52)	4	7.23 (6.78 - 7.67)	3	6.90 (6.31 - 7.30)	3	7.19 (6.85 - 7.51)	3
CDPPB	6.49 (6.00 - 6.98)	4	n.a.	3	6.57 (6.32 - 6.81)	3	5.63 (5.35 - 6.07)	3
compound 2c	5.40 (4.89 - 5.91)	4	n.a.	3	5.88 (5.58 - 6.19)	3	4.86 (4.62 - 5.13)	3
DHPG								
MPPA	6.72 (6.34 - 7.10)	4	6.22 (5.76 - 6.67)	3	6.60 (6.12 - 7.07)	3	6.55 (6.20 - 6.90)	3
CDPPB	6.67 (6.20 - 7.08)	4	n.a.	3	6.37 (6.02 - 6.72)	3	6.34 (6.12 - 6.57)	3
compound 2c	5.30 (4.90 - 6.03)	4	n.a.	3	5.40 (4.59 - 6.22)	3	4.50 (4.32 - 4.69)	3

n.a. Due to full agonist activity of CDPPB in IP_1 accumulation assays, it was not possible to fit the operational model of allosterism to PAM titration curves in the presence of EC_{20} orthosteric agonist. Compound 2c potentiated orthosteric agonist activity for IP_1 accumulation above the maximal agonist response, prohibiting accurate estimation of pK_B as there was no independent means to determine the maximal system response (E_m).

[a]Select PAMs potentiated orthosteric agonist-induced internalization above the maximum achieved by orthosteric agonist alone. In order to fit the operational model, the E_m was constrained to the maximum level of potentiation observed in the presence of PAM (143% for glutamate and 210% for DHPG).

[b]pK_B, negative logarithm of the dissociation binding constant determined with the operational model of allosterism, for each modulator. None of the pK_B estimates determined from interactions with the same orthosteric agonist had $P < 0.05$ (one-way ANOVA with Tukey's multiple comparisons test).

Table 4

Cooperativity factors for allosteric modulation of low concentrations of orthosteric ligand (L-glutamate or DHPG) by $mGlu_5$ PAMs in HEK293A-$mGlu_5$-low or HEK293A cells. Data represent the mean and 95% CI of *n* independent experiments performed in triplicate.

	Ca^{2+} mobilization		**IP_1 accumulation**		**pERK1/2**		**Internalization[a]**	
Ligand	*logβ[b] (95% CI)*	*n*	*logβ (95% CI)*	*n*	*logβ (95% CI)*	*n*	*logβ (95% CI)*	*n*
L-glutamate								
MPPA	0.73 (0.57 - 0.89)	4	0.19 (0.15 - 0.24)[e]	3	0.34 (0.28 - 0.41)[e]	3	0.18 (0.16 - 0.21)[e]	3
CDPPB	0.39 (0.20 - 0.58)	4	n.a.	3	0.16 (0.04 - 0.28)	3	0.44 (0.29 - 0.75)	3
compound 2c	0.87 (0.63 - 1.11)	4	n.a.	3	0.48 (0.42 - 0.55)	3	0.48 (0.41 - 0.59)	3
DHPG								
MPPA	1.04 (0.88 - 1.24)	4	0.45 (0.28 - 0.62)[e,f]	3	0.94 (0.80 - 1.09)	3	0.40 (0.35 - 0.45)[e,f]	3
CDPPB	0.71[g] (0.54 - 0.91)	4	n.a.	3	0[c]	3	0[c]	3
compound 2c	1.40 (1.14 - 1.99)	4	n.a.	3	1.23 (0.76 - 1.70)	3	0.98 (0.89 - 1.08)	3

n.a. Due to full agonist activity of CDPPB in IP_1 accumulation assays it was not possible to fit the operational model of allosterism to PAM titration curves in the presence of EC_{20} orthosteric agonist. Compound 2c potentiated orthosteric agonist activity for IP_1 accumulation above the maximal agonist response, prohibiting accurate estimation of logβ as there was no independent means to determine the maximal system response (E_{max}).

[a]Select PAMs potentiated orthosteric agonist-induced internalization above the maximum achieved by orthosteric agonist alone. In order to fit the operational model, the E_m was constrained to the maximum level of potentiation observed in the presence of PAM (143% for glutamate and 210% for DHPG).

[b]logβ, logarithm of the efficacy cooperativity factor.

[c]An F-test revealed that logβ was not different from 0 and logβ was therefore constrained to 0. As such the observed response is assumed to be a combination of the orthosteric ligand and the intrinsic agonist activity of CDPPB where log(τ_B) was equal to -0.49 (Ca^{2+}), -0.11 (pERK1/2), -0.02 (internalization) based on intrinsic agonism in the presence of LY341495.

[e]$P < 0.05$ when compared with estimate from Ca^{2+} mobilization by one-way ANOVA with Tukey's multiple comparisons test.

[f]$P < 0.05$ when compared with estimate from pERK1/2 by one-way ANOVA with Tukey's multiple comparisons test.

[g]$P < 0.05$ when compared with 0 (one-sample t-test).

Table 5

Quantification of agonist activity of DHPG or PAMs, as well as PAM modulation of DHPG responses, in mouse cortical neurons. Data represent the mean and 95% CI of n independent experiments performed in duplicate.

	Ca^{2+} mobilization						**IP_1 accumulation**					
Ligand	*pK_A[a] (95% CI)*	*$log(\tau/K_A)$[b] (95% CI)*	*n*	*pK_B[c] (95% CI)*	*$log\beta$[d] (95% CI)*	*n*	*pK_A (95% CI)*	*$log(\tau/K_A)$ (95% CI)*	*n*	*pK_B (95% CI)*	*$log\beta$ (95% CI)*	*n*
DHPG	n.d.	6.42 (6.34 - 6.49)	9	-	-	-	n.d.	5.70 (5.47 - 5.95)	8	-	-	-
MPPA	n.r.	n.r.	6	6.74 (5.74 - 7.70)	0.45[e] (0.32 - 0.58)	5	6.38 (5.81 - 6.88)	6.47 (6.12 - 6.96)	5	6.53 (6.01 - 7.06)	0[f]	4
CDPPB	n.r.	n.r.	6	7.22 (6.70 - 7.76)	0.53[e] (0.41 - 0.67)	5	6.48 (6.02 - 6.90)	6.74 (6.48 - 7.11)	6	6.43 (6.00 - 6.86)	0	4
compound 2c	5.84 (4.42 - 6.73)	5.49 (4.73 - 6.80)	7	6.26 (5.84 - 7.29)	0.94[e] (0.67 - 1.81)	7	5.23 (4.59 - 6.00)	5.35 (4.80 - 5.81)	6	6.03 (5.43 - 6.78)	0	6

n.d. not determined; n.r. no response

[a]pK_A, negative logarithm of the equilibrium dissociation binding constant determined with the operational model of agonism. The pK_A values for compound 2c in the two assays had $P > 0.05$ (two-tailed unpaired t-test).

[b]$\log(\tau/K_A)$, transduction coefficient; τ, intrinsic efficacy. The $\Delta\log(\tau/K_A) = \log(\tau/K_A)_{DHPG} - \log(\tau/K_A)_{PAM}$ values for compound 2c in the two assays had $P > 0.05$ (two-tailed unpaired t-test).

[c]pK_B, negative logarithm of the dissociation binding constant determined with the operational model of allosterism. The pK_B values determined for the same compound in the two assays had $P > 0.05$ (two-tailed unpaired t-test).

[d]logβ, logarithm of the efficacy cooperativity factor.

[e]$P < 0.05$ when compared with 0 (one-sample t test).

[f]For fits where logβ was not different from 0 (determined by F-test) logβ was constrained to 0, assuming that the observed response is due to a combination of the orthosteric ligand and the intrinsic agonist activity of the PAM.

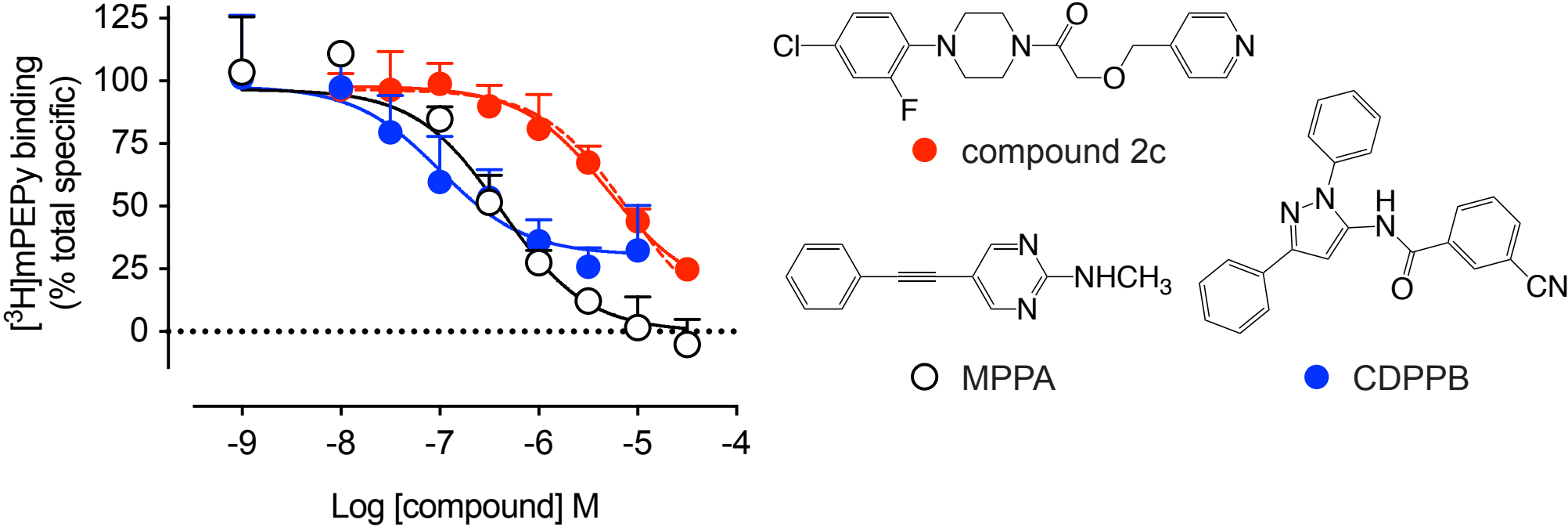
125
100
75
50
25
0
[3H]mPEPy binding
(% total specific)
-9
-8
-7
-6
-5
-4
Log [compound] M
Cl
F
N
N
O
O
N
compound 2c
N
N
NHCH3
MPPA
N
N
H
N
O
CN
CDPPB

Figure 1

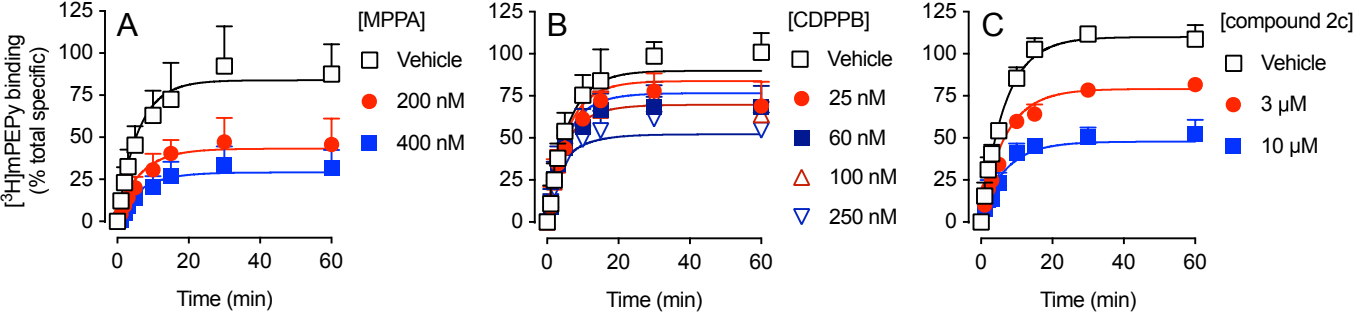
A
B
C
[^{3}H]mPEPy binding
(% total specific)
125
100
75
50
25
0
0
20
40
60
Time (min)
[MPPA]
Vehicle
200 nM
400 nM
[CDPPB]
Vehicle
25 nM
60 nM
100 nM
250 nM
[compound 2c]
Vehicle
3 μM
10 μM

Figure 2

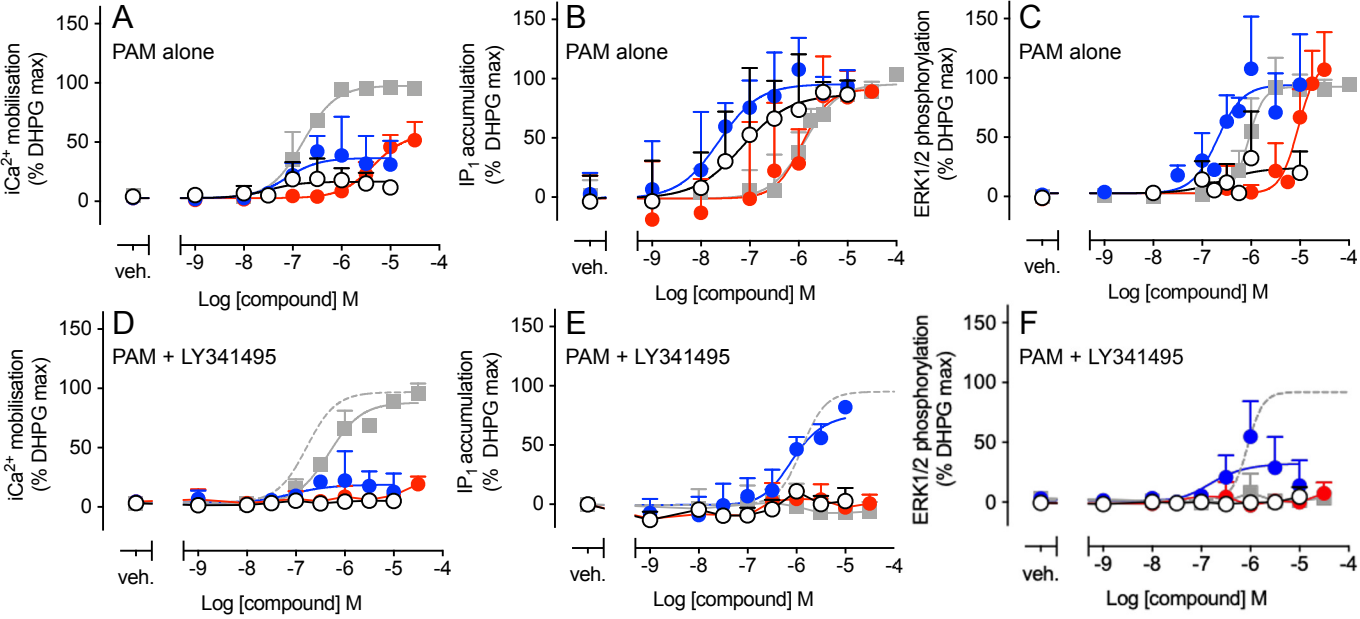
A
PAM alone
iCa2+ mobilisation (% DHPG max)
B
PAM alone
IP1 accumulation (% DHPG max)
C
PAM alone
ERK1/2 phosphorylation (% DHPG max)
D
PAM + LY341495
iCa2+ mobilisation (% DHPG max)
E
PAM + LY341495
IP1 accumulation (% DHPG max)
F
PAM + LY341495
ERK1/2 phosphorylation (% DHPG max)
150
100
50
0
veh.
-9
-8
-7
-6
-5
-4
Log [compound] M
DHPG
MPPA
CDPPB
compound 2c

Figure 3

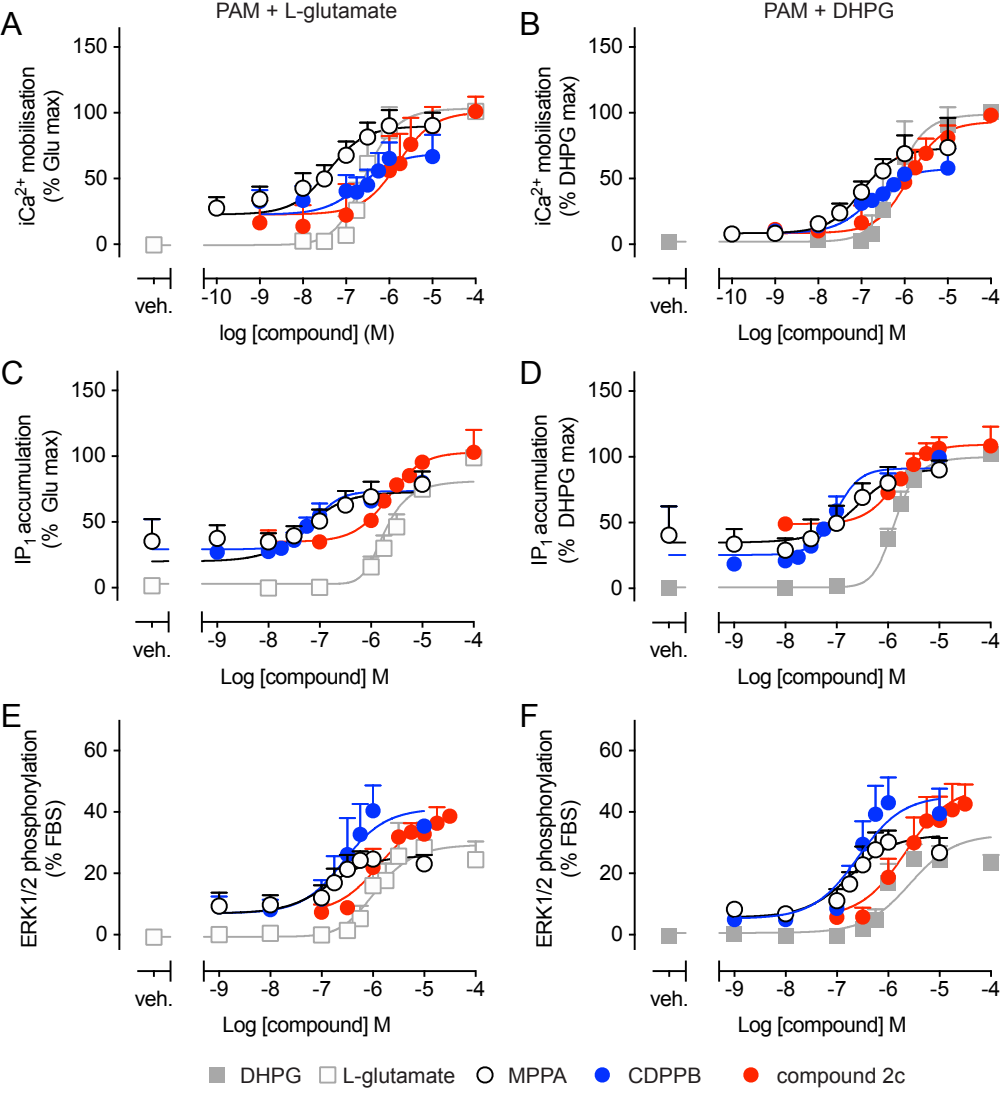
A
PAM + L-glutamate
B
PAM + DHPG
iCa2+ mobilisation (% Glu max)
iCa2+ mobilisation (% DHPG max)
C
D
IP1 accumulation (% Glu max)
IP1 accumulation (% DHPG max)
E
F
ERK1/2 phosphorylation (% FBS)
veh.
log [compound] (M)
Log [compound] M
DHPG
L-glutamate
MPPA
CDPPB
compound 2c

Figure 4

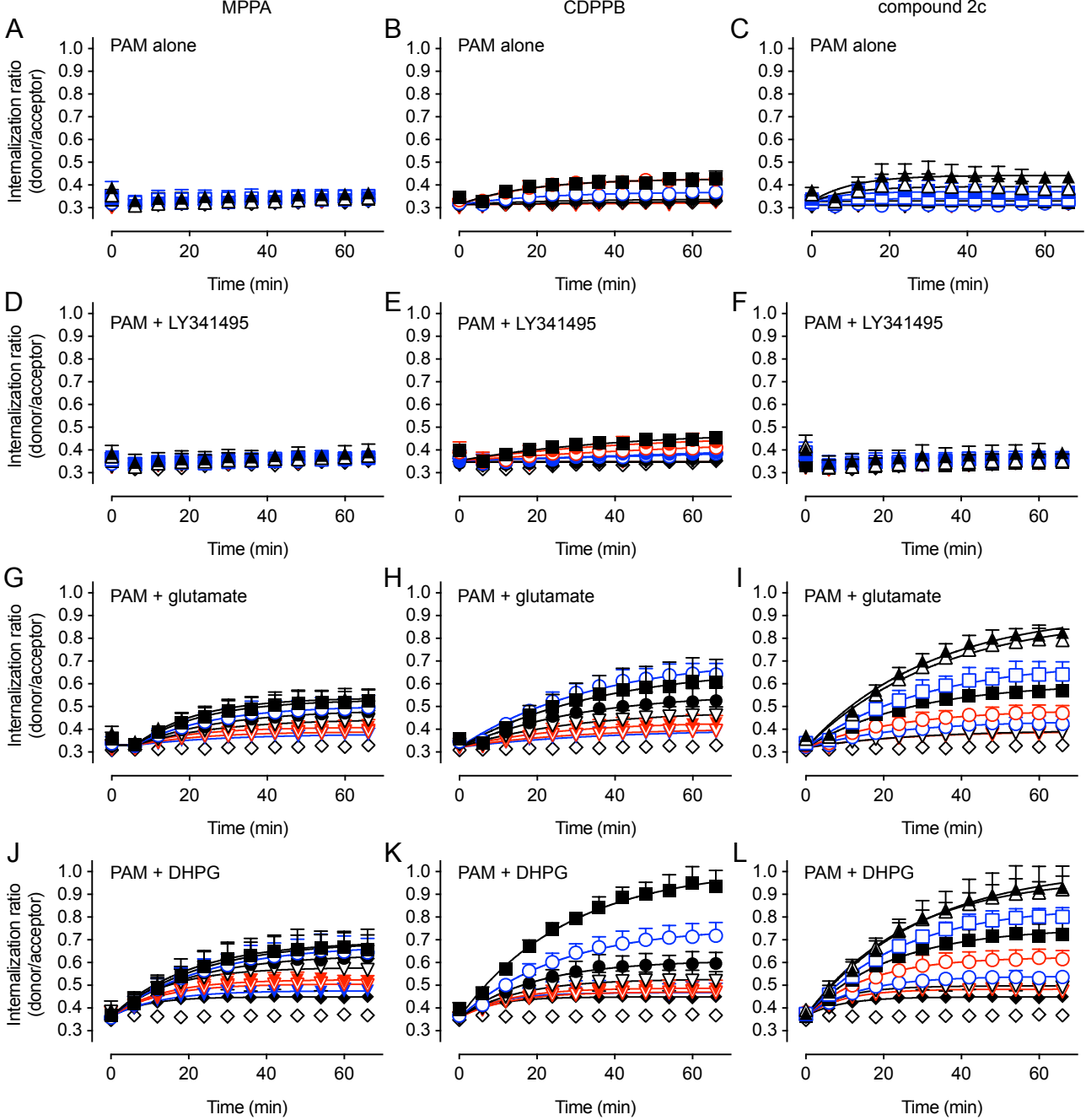
MPPA
CDPPB
compound 2c
A
B
C
D
E
F
G
H
I
J
K
L
PAM alone
PAM + LY341495
PAM + glutamate
PAM + DHPG
Internalization ratio (donor/acceptor)
Time (min)
Vehicle
TBOA
1 nM
10 nM
32 nM
100 nM
316 nM
1 μM
1.8 μM
3.2 μM
5.6 μM
10 μM
18 μM
32 μM
56 μM
100 μM

Figure 5

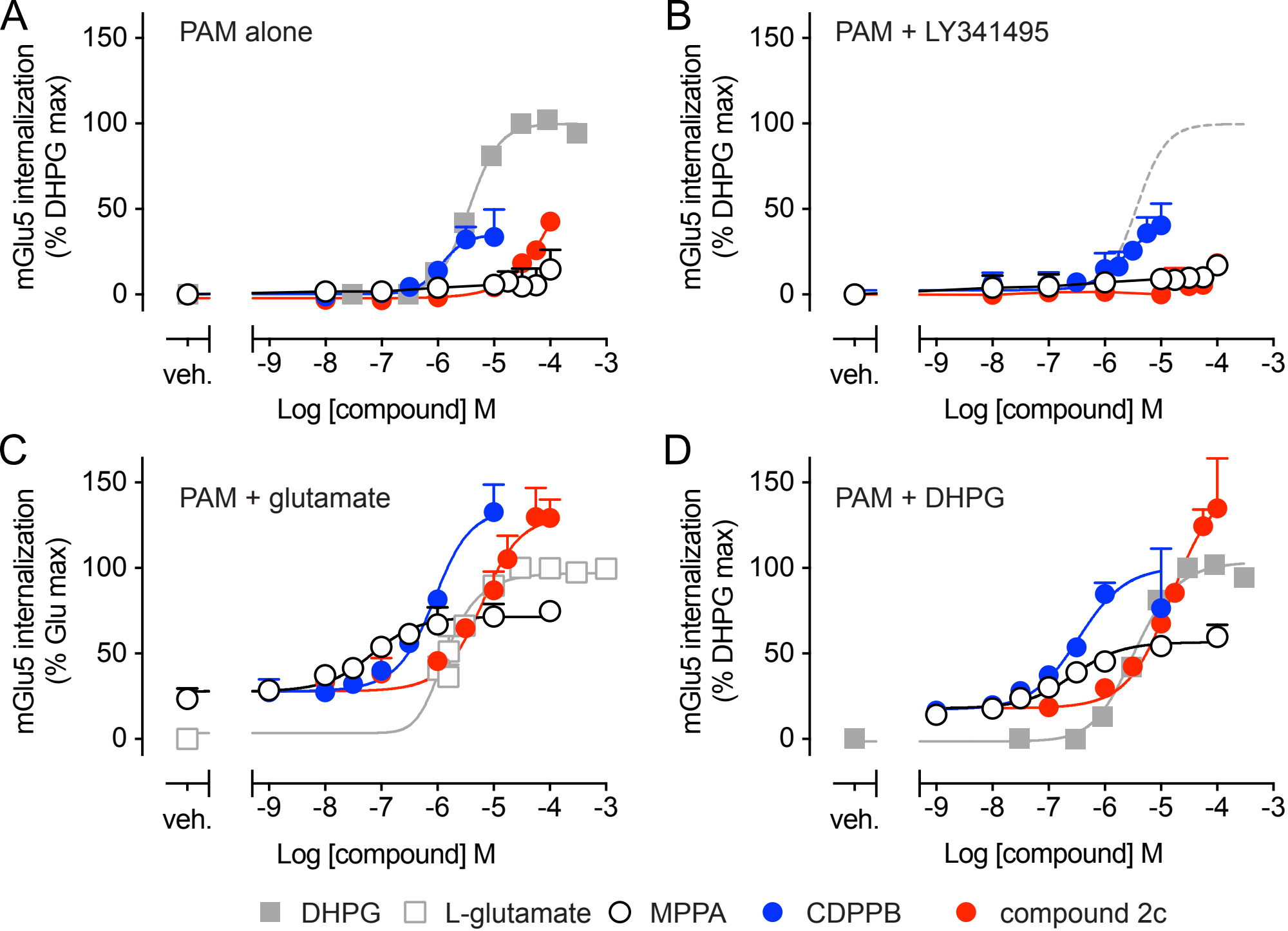
A
PAM alone
mGlu5 internalization (% DHPG max)
150
100
50
0
veh.
-9
-8
-7
-6
-5
-4
-3
Log [compound] M
B
PAM + LY341495
mGlu5 internalization (% DHPG max)
C
PAM + glutamate
mGlu5 internalization (% Glu max)
D
PAM + DHPG
mGlu5 internalization (% DHPG max)
DHPG
L-glutamate
MPPA
CDPPB
compound 2c

Figure 6

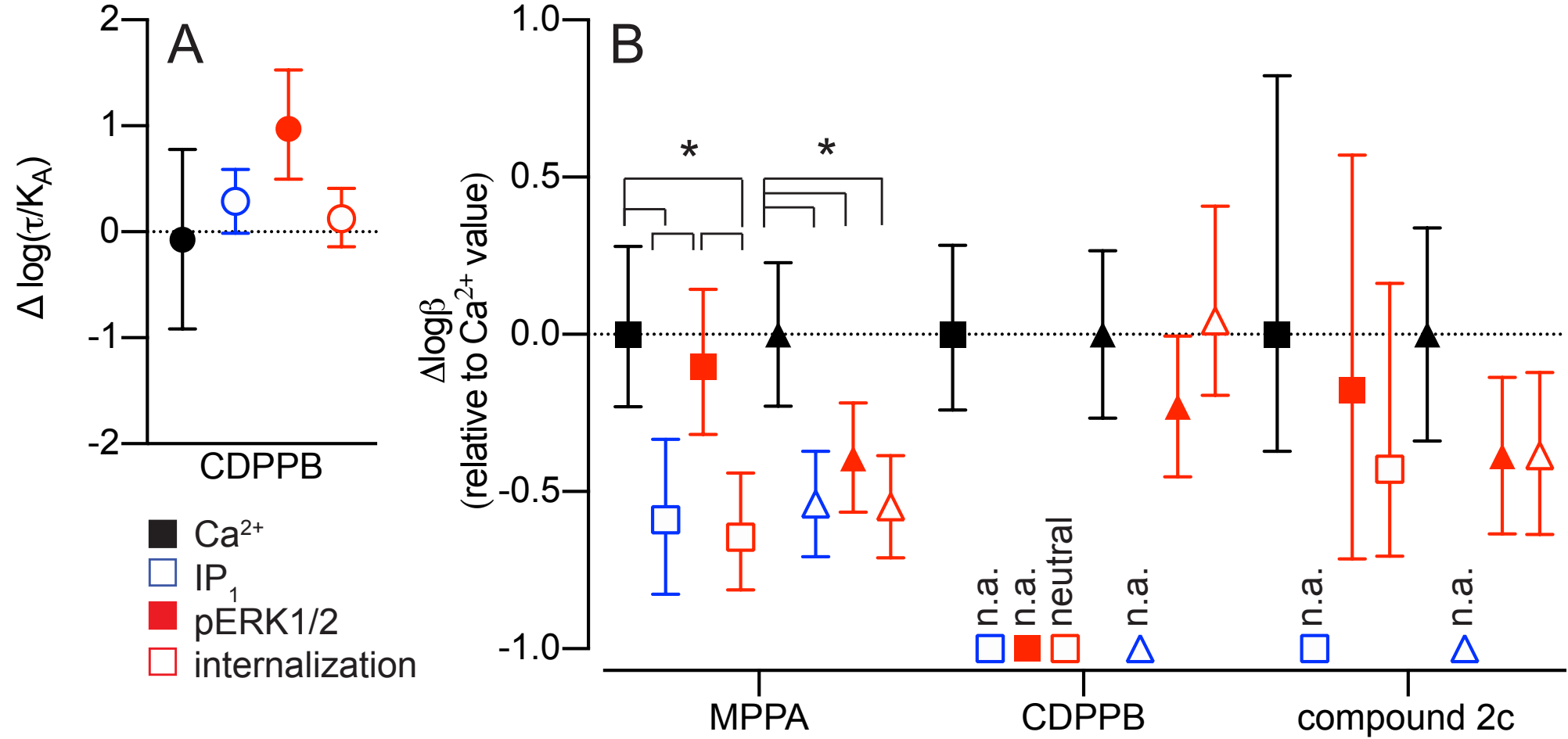
A
2
1
0
-1
-2
Δ log(τ/K_A)
CDPPB
Ca2+
IP1
pERK1/2
internalization
B
1.0
0.5
0.0
-0.5
-1.0
Δlogβ
(relative to Ca2+ value)
*
*
n.a.
n.a.
neutral
n.a.
n.a.
n.a.
MPPA
CDPPB
compound 2c

Figure 7

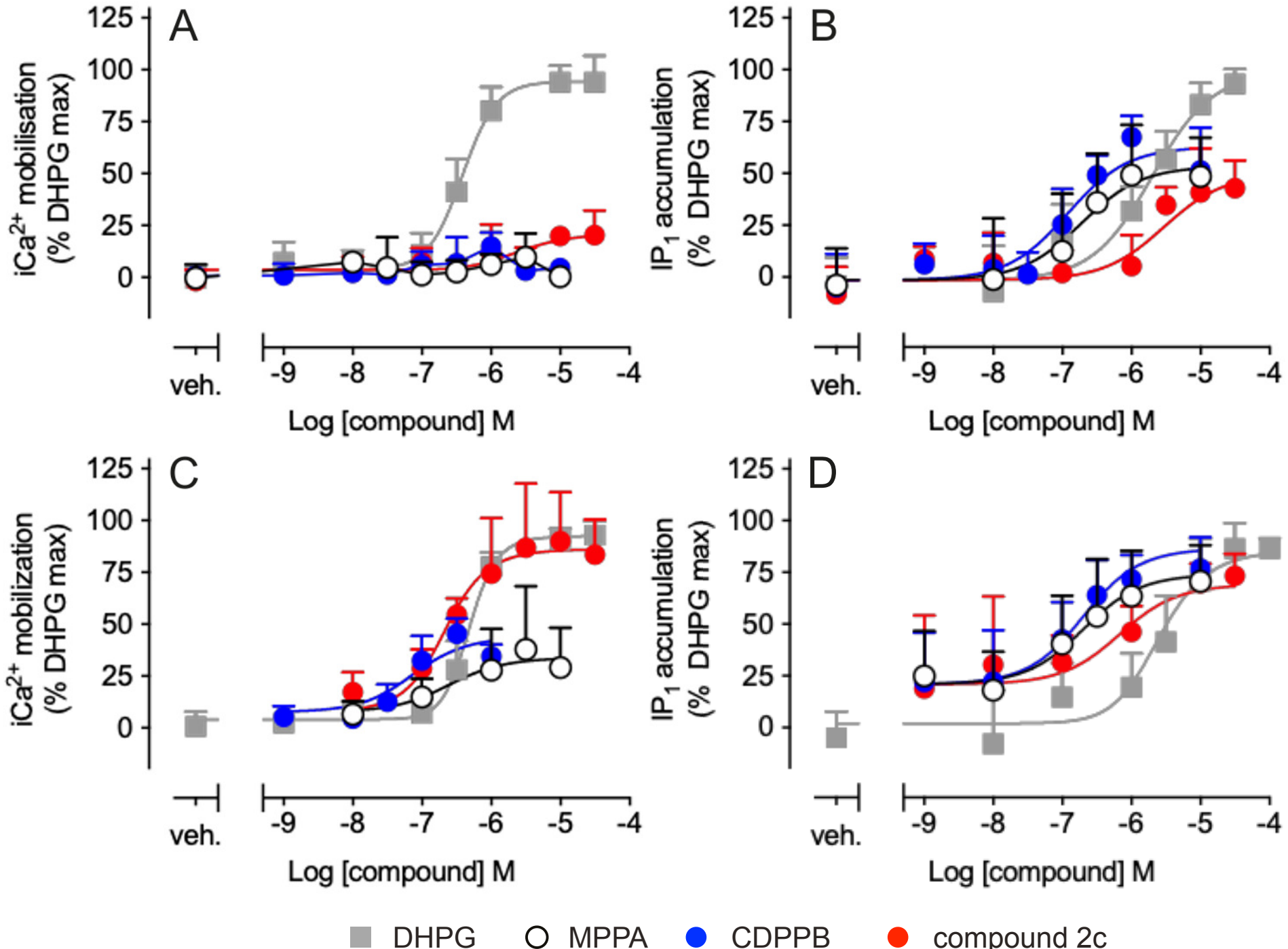
A
B
C
D
iCa2+ mobilisation (% DHPG max)
IP1 accumulation (% DHPG max)
iCa2+ mobilization (% DHPG max)
125
100
75
50
25
0
veh.
-9
-8
-7
-6
-5
-4
Log [compound] M
DHPG
MPPA
CDPPB
compound 2c

Figure 8